The neocortex of cetartiodactyls. II. Neuronal morphology of the visual and motor cortices in the giraffe (Giraffa camelopardalis)

ARTICLE *in* BRAIN STRUCTURE AND FUNCTION · JULY 2014

Impact Factor: 5.62 · DOI: 10.1007/s00429-014-0830-9 · Source: PubMed

9 AUTHORS, INCLUDING:

Bob Jacobs
Colorado College
38 PUBLICATIONS **1,405** CITATIONS
SEE PROFILE

Camilla Butti
Icahn School of Medicine at Mount Sinai
27 PUBLICATIONS **480** CITATIONS
SEE PROFILE

Chet C Sherwood
George Washington University
133 PUBLICATIONS **2,536** CITATIONS
SEE PROFILE

Paul Manger
University of the Witwatersrand
170 PUBLICATIONS **2,956** CITATIONS
SEE PROFILE

Brain Struct Funct
DOI 10.1007/s00429-014-0830-9

ORIGINAL ARTICLE

The neocortex of cetartiodactyls. II. Neuronal morphology of the visual and motor cortices in the giraffe (*Giraffa camelopardalis*)

Bob Jacobs · Tessa Harland · Deborah Kennedy · Matthew Schall · Bridget Wicinski · Camilla Butti · Patrick R. Hof · Chet C. Sherwood · Paul R. Manger

Received: 11 May 2014 / Accepted: 21 June 2014

Abstract The present quantitative study extends our investigation of cetartiodactyls by exploring the neuronal morphology in the giraffe (*Giraffa camelopardalis*) neocortex. Here, we investigate giraffe primary visual and motor cortices from perfusion-fixed brains of three subadults stained with a modified rapid Golgi technique. Neurons ($n = 244$) were quantified on a computer-assisted microscopy system. Qualitatively, the giraffe neocortex contained an array of complex spiny neurons that included both "typical" pyramidal neuron morphology and "atypical" spiny neurons in terms of morphology and/or orientation. In general, the neocortex exhibited a vertical columnar organization of apical dendrites. Although there was no significant quantitative difference in dendritic complexity for pyramidal neurons between primary visual ($n = 78$) and motor cortices ($n = 65$), there was a significant difference in dendritic spine density (motor cortex > visual cortex). The morphology of aspiny neurons in giraffes appeared to be similar to that of other eutherian mammals. For cross-species comparison of neuron morphology, giraffe pyramidal neurons were compared to those quantified with the same methodology in African elephants and some cetaceans (e.g., bottlenose dolphin, minke whale, humpback whale). Across species, the giraffe (and cetaceans) exhibited less widely bifurcating apical dendrites compared to elephants. Quantitative dendritic measures revealed that the elephant and humpback whale had more extensive dendrites than giraffes, whereas the minke whale and bottlenose dolphin had less extensive dendritic arbors. Spine measures were highest in the giraffe, perhaps due to the high quality, perfusion fixation. The neuronal morphology in giraffe neocortex is thus generally consistent with what is known about other cetartiodactyls.

Keywords Dendrite · Morphometry · Dendritic spine · Golgi method · Brain evolution

B. Jacobs (✉) · T. Harland · D. Kennedy · M. Schall
Laboratory of Quantitative Neuromorphology, Psychology, Colorado College, 14 E. Cache La Poudre, Colorado Springs, CO 80903, USA
e-mail: bjacobs@coloradocollege.edu

B. Wicinski · C. Butti · P. R. Hof
Fishberg Department of Neuroscience and Friedman Brain Institute, Mount Sinai School of Medicine, One Gustave L. Levy Place, New York, NY 10029, USA

C. C. Sherwood
Department of Anthropology, The George Washington University, 2110 G Street, NW, Washington, DC 20052, USA

P. R. Manger
School of Anatomical Sciences, Faculty of Health Sciences, University of the Witwatersrand, 7 York Road, Parktown, Johannesburg 2193, South Africa

Introduction

In our companion paper on cetartiodactyls (Butti et al. 2014b), we documented the neuronal morphology of three cetacean species (bottlenose dolphin, minke whale, and humpback whale). Here, we explore the neuronal morphology of the giraffe (*Giraffa camelopardalis*) for the first time. Although the long necked-giraffe's status as the tallest extant land mammal has resulted in extensive investigation of its vertebral column (Solounias 1999; Badlangana et al. 2009) and cardiovascular system (Nilsson et al. 1988; Badeer 1997), few studies have examined the giraffe brain beyond gross anatomy (Friant 1968). Recent investigations have begun to explore the

Published online: 22 July 2014

implications of an elongated neck in the anatomy of brainstem nuclei (Badlangana et al. 2007a; Bux et al. 2010) and the corticospinal system (Badlangana et al. 2007b); nevertheless, apart from some initial descriptions of neurons in selected ungulates (Barasa 1960), the morphology of cortical neurons in the giraffe remains unknown. As part of an ongoing project documenting neocortical neuromorphology in previously unexplored large brained mammals (Jacobs et al. 2011), the current study may further our understanding of which aspects of neuronal morphology are general to all vertebrates, and which are specific to particular species. To that end, the present investigation documents the neuronal morphology of the primary motor and visual cortices of the giraffe.

Within the superorder Laurasiatheria, giraffes belong to the clade Cetartiodactyla (order Artiodactyla; suborder Ruminantia). Giraffidae emerged from Pecora in the Oligocene period, with Giraffini diverging from their closest living relative, Okapini, approximately 19 million years ago (Hassanin and Douzery 2003). Extant laurasiatherian species (e.g., giraffe, cat, dog, horse, sheep, cow, seal, hippopotamus, dolphin, whale) exhibit considerable diversity in terms of physiology, behavior, brain mass, and encephalization quotient (Radinsky 1981; Fernández and Vrba 2005; Boddy et al. 2012), and thus may provide insight into the complexities and evolutionary plasticity of mammalian neocortical evolution. In particular, comparison of evolutionary patterns and modern phylogenomic techniques underscore a close relationship between cetaceans and artiodactyls, which have recently been grouped in the clade Cetartiodactyla (Nikaido et al. 1999; Murphy et al. 2004; Price et al. 2005). It should be noted that the Artiodactyla suborder Ruminantia appears to be most closely related to hippopotami and cetaceans, and composes a clade referred to as Cetruminantia (Graur and Higgins 1994; Shimamura et al. 1997). As such, it would be reasonable to expect similarities in the organization of the brain among related species within cetartiodactyls (Hof and Sherwood 2005, 2007; Sherwood et al. 2009). For example, in the pygmy hippopotamus (*Hexaprotodon liberiensis*) and cetaceans (bottlenose dolphin, *Tursiops truncatus*; minke whale, *Balaenoptera acutorostrata*; humpback whale, *Megaptera novaeangliae*), a variety of complex neocortical neurons have recently been documented, with spiny neurons existing along a continuum from those that appeared more pyramid-like to those that differ from the "typical" (i.e., primate/rodent-like) pyramidal neuron in terms of morphology and/or orientation (Butti et al. 2014a, b). In contrast, aspiny cortical neurons appear relatively uniform and morphologically conserved across eutherian mammals (Hof et al. 1999; Sherwood et al. 2009). Given the close relationship between certain large artiodactyls (e.g., Hippopotomidae) and cetaceans (Shimamura et al. 1997; Ursing and Arnason 1998; Nikaido et al. 1999; Price et al. 2005), we expect comparable neuromorphological features across giraffes, the pygmy hippopotamus, and cetaceans. Such a comparative perspective provides a focal point of the current investigation.

The giraffe, with a brain mass of between 400 and 700 g (Crile and Quiring 1940; Mitchell et al. 2008), has a relatively long gestation period and a relatively complex sociobehavioral environment (Pérez-Barbería and Gordon 2005; Shultz and Dunbar 2006). They reside within a fission–fusion, mostly matrilineal social structure characterized by considerable flexibility in herd size (Van der Jeugd and Prins 2000; Bashaw et al. 2007; Bercovitch and Berry 2013; Carter et al. 2012). Several types of social interaction have been documented: urine assessment to determine female reproductive status, mate guarding of receptive females (Bercovitch et al. 2006), and neck rubbing for social cohesion and bonding (Coe 1967; Tarou et al. 2000). Auditory and particularly visual senses seem well developed (Innis 1958). The giraffe has a visual acuity of 25–27 cycles per degree, which is approximately half that of humans, but substantially higher than that seen in most other Cetartiodactyls (Coimbra et al. 2013). The extent to which giraffes communicate vocally remains unclear, although it has been suggested that they are among several species (e.g., okapi, rhinoceros, elephants, whales) that may use infrasound (Bashaw 1993). These behaviors, coupled with a relatively large brain size, suggest considerable cognitive ability in giraffes.

The relationship between cognitive abilities and cortical neuronal morphometry remains elusive in giraffes because their cerebral cortex remains largely unexplored (DeFelipe et al. 2002), with only one recent study examining giraffe cortex directly (Badlangana et al. 2007b). Therefore, in addition to qualitative classification of neuronal types, the present study quantitatively investigated regional variation, with a focus on the numerically dominant pyramidal neurons, in primary motor and visual cortices. Although increased dendritic complexity has been associated with enhanced processing demands in higher order primate cortices (Elston 2003, 2007; Jacobs and Scheibel 2002), there appears to be no a priori reason to expect differences in cortical processing across primary cortical areas (Jacobs et al. 2001; Clemo and Meredith 2012). As such, we expect pyramidal neuron dendritic extent to be similar between giraffe primary motor and visual cortices.

Materials and methods

Specimens

Tissue was obtained from three (G1, G2, G3) subadult male giraffes (2–4 years of age) euthanized with an intravenous overdose of sodium pentobarbital (for details, see Dell et al. 2012). Briefly, after being perfused through the common carotid artery with 0.9 % saline solution and a fixative of 4 % paraformaldehyde in 0.1 M phosphate buffer, each brain was placed in fixative, weighed (G1: 610 g, G2: 527 g, G3: 480 g), and post-fixed in 4 % paraformaldehyde in 0.1 M phosphate buffer (Manger et al. 2009). In postmortem examinations, the brains of all animals exhibited no obvious gross neuroanatomical abnormalities. Tissue blocks (3–5 mm-thick) were dissected from the cortical surface and stored in 1 % sodium azide in 0.1 M phosphate buffer for 3 months prior to staining. The present study was approved by the Colorado College Institutional Review Board (#011311-1) and the University of the Witwatersrand Animal Ethics Committee (2008/36/1).

Tissue selection

Cortical blocks (3–5 mm-thick) were removed from the right hemisphere. Tissue from the primary motor cortex, located anteriorly on the dorsomedial aspect of the neocortex (Badlangana et al. 2007b), was removed approximately 1–2 cm lateral to the longitudinal fissure; tissue from the primary visual cortex, located posteriorly on the dorsomedial aspect of the neocortex, was removed approximately 2–3 cm lateral to the longitudinal fissure (Fig. 1). Tissue was coded to prevent experimenter bias, stained via a modified rapid Golgi technique (Scheibel and Scheibel 1978b), and sectioned serially at 120 μm with a vibratome (Leica VT1000S, Leica Microsystems, Buffalo Grove, IL, USA). Tissue blocks adjacent to those removed for Golgi analysis were examined with a routine Nissl and myelin stain to reveal cytoarchitectonic characteristics. To determine laminar thickness, sample measurements for each layer were averaged in Nissl stains across 10 sections from each cortical region.

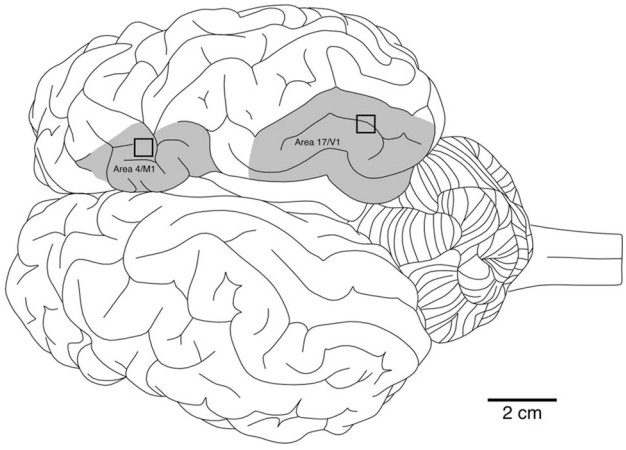

Fig. 1 Dorsal view of a giraffe brain illustrating the primary motor and visual cortices from which tissue blocks were selected for staining. Adapted from Fig. 2 in Badlangana et al. (2007b)

Neuron selection and quantification

Neurons ($n = 244$) were analyzed across the three giraffes from motor ($n = 125$: G1, 78; G2, 11; G3, 36) and visual cortices ($n = 119$; G1, 67; G2, 13; G3, 39), with more neurons from G1 ($n = 145$) and G3 ($n = 75$) than from G2 ($n = 24$) due to inconsistent staining. Neurons were selected for tracing based on established criteria (Roitman et al. 2002; Anderson et al. 2009; Jacobs et al. 2011; Lu et al. 2013), which required an isolated soma near the center of the 120 μm section, with as fully impregnated, unobscured, and complete dendritic arbors as possible (i.e., no beading or interruptions). To provide a comprehensive analysis of giraffe neuromorphology, neurons were selected to encompass representative typologies, and were quantified under a planachromatic 60× oil objective (NA 1.4) along *x*-, *y*-, *z*-coordinates using a Neurolucida system (MBF Bioscience, Williston, VT, USA) interfaced with an Olympus BH-2 microscope equipped with a Ludl XY motorized stage (Ludl Electronics, Hawthorne, NY, USA) and a Heidenhain *Z*-axis encoder (Schaumburg, IL, USA). A MicroFire Digital CCD 2-megapixel camera (Optronics, Goleta, CA, USA) mounted on a trinocular head (model 1-L0229, Olympus, Center Valley, PA, USA) displayed images on a 1,920 × 1,200 resolution Dell E248WFP 24-in. LCD monitor. Somata were traced first at their widest point in the two-dimensional plane to provide an estimate of the cross-sectional area. Subsequently, dendrites were traced somatofugally in their entirety, recording dendritic diameter and quantity of spines, without differentiating morphological types of spines. Dendritic arbors were not followed into adjacent sections, with broken ends and ambiguous terminations identified as incomplete endings.

Neurons were traced by two investigators (TH and DK). Intrarater reliability was determined by having each rater trace the same soma, dendritic segment, and spines 10 times. The average coefficient of variation for soma size (3.8 %), dendritic spine number (DSN 7.2 %) and total dendritic length (TDL 3.9 %) indicated little variation in the tracings. Intrarater reliability was further tested with a split plot design ($\alpha = 0.05$), which indicated no significant difference between the first five tracings and the last five

tracings. Interrater reliability was determined through comparison of 10 dendritic system tracings with the same tracings completed by the primary investigator (BJ). Interclass correlations across soma size, DSN, and TDL averaged 0.98, 0.95, 0.99, respectively. An analysis of variance (ANOVA, $\alpha = 0.05$) indicated no significant differences among the tracers for the three measures. Additionally, the primary investigator reexamined all completed tracings under the microscope to ensure accuracy.

Neuron descriptions and dependent dendritic/spine measures

Descriptively, neurons were classified according to somatodendritic criteria (Ferrer et al. 1986a, b; Jacobs et al. 2011) by considering factors such as soma size/shape, presence of spines, laminar location, and general morphology. Quantitatively, centrifugal nomenclature was used to characterize branches extending from the soma as first-order segments, which bifurcate into second- and then third-order segments, and so on (Bok 1959; Uylings et al. 1986). In addition to quantifying soma size (i.e., surface area, μm^2) and depth from the pial surface (μm), we examined six other measures that have been analyzed in previous studies (Jacobs et al. 2011): dendritic volume (Vol μm^3, the total volume of all dendrites); total dendritic length (TDL μm, the summed length of all dendritic segments); mean segment length (MSL μm, the average length of each dendritic segment); dendritic segment count (DSC, the number of dendritic segments); dendritic spine number (DSN, the total number of spines on dendritic segments); and dendritic spine density (DSD, the average number of spines per μm of dendritic length). Additionally, dendritic branching patterns were analyzed using a Sholl analysis (Sholl 1953), which quantified dendritic intersections at 20-μm intervals radiating somatofugally. All descriptive measures are presented as mean ± standard deviation (SD) unless noted otherwise (e.g., Table 3).

Independent variables and statistical analyses

Descriptive statistics obtained for the six dependent measures were aggregated by neuron type and brain region. For inferential statistical analysis of regional dendritic differences, only pyramidal neurons were examined (using SPSS release 19.0.0.1), with dendritic systems as the unit of analysis. In the past, we have used a nested repeated measures design (PROC NESTED; SAS) to analyze regional cortical dendritic differences. The present study, however, expanded this analysis by incorporating the main effects of three Brains (G1, $n = 88$ pyramidal neurons; G2, $n = 7$ pyramidal neurons; G3, $n = 48$ pyramidal neurons) and the nested effect of two Regions (motor and visual cortices) within Brain. Three subsequent levels of analysis were completed: (1) a cluster analysis to provide an initial descriptive overview of dendritic distributions, (2) a series of decision trees to explore potentially significant relationships between Brain and Region for each dependent measure, and (3) a generalized linear equations (GENLIN) framework to assess whether overall variability in the measure could be modeled. Each of these is explained in detail below.

Insofar as dendritic measures may be distributed differently within nested effects, a two-stage cluster analysis of Brains, and Regions nested within Brains, was performed using Akaike's Information Criteria for Brains G1 and G3 with both Brain, and Region within Brain entered as effects and a forced solution of four clusters. For this cluster analysis, Brain G2 was excluded due to a small sample size. Within each cluster, dependent variable distributions were examined to characterize the data. Log-likelihood distances were used with standardization of the dependent measures to define similarity.

Because brains may differ from each other for a variety of reasons, a CHAID decision tree framework (Hawkins and Kass 1982), with a parent node size set to 20 and child node size set to 10 with Brain forced in as the first effect and Block nested within Brain as the second effect, was used to explore possible asymmetric effects such as differential relevance of Block within Brain. This analysis was chosen because the three Brains could have differences in their structures that would not be apparent from conventional t tests or an ANOVA. In addition, this form of analysis is crucial for understanding results with small sample sizes and reveals which Brains were similar/different from each other. Specifically, possible differences were evaluated for (1) Brain main effect with six tests across the 2 Brains on the 6 dendritic measures and (2) the Region within Brain effect with 18 tests across 2 Regions evaluated for 6 dependent measures across 3 Brains.

To summarize the relationships between the dependent variables, and the nested and main effects, a bootstrap of 100 runs was used to secure robust maximum likelihood estimations (RMLE) within the analytical framework of GENLIN tested with a variety of links and distributions. GENLIN enables analyses that separate distributional characteristics of the dependent measures (e.g., normal versus probit) from the transformation used to estimate the model (e.g., identity or no transformation, Cauchit for a multinomial mixture). A variety of distribution and link functions were evaluated after examining the descriptive results. The small sample size warranted the use of the

bootstrap estimations of RMLE effects. Six such analyses, one for each dependent variable, were performed, with five χ^2 statistics calculated for each model: (1) improvement over a model fit with just the intercept term, (2) overall goodness of fit and three significance tests of the (3) intercept, (4) Brain and (5) Region nested within Brain.

Results

Overview

Nissl and myelin stains suggested an absence of a clear layer IV in the primary motor cortex, but not in primary visual cortex (Fig. 2). The relative thickness of all laminae across both cortical regions is provided in Table 1, with layers I and III in both regions being relatively thick. The overall high quality of Golgi preparations is evident in photomicrographs (Figs. 3, 4), which reveal well impregnated, relatively complete dendritic systems. In general, pyramidal-like neurons in both regions exhibited long (up to ~1,500 μm) apical dendrites which, in extending up to layers I and II, contributed to the vertical, columnar organization of the neocortex. Aspiny neurons were found at all depths, with considerable variation in dendritic density and length. Quantitative data broken down by cortical region and neuron type are presented in Table 2, which indicates that spiny neurons in motor cortex (excluding the gigantopyramidal neurons found only in motor cortex) tended to exhibit greater dendritic (by 39 % for Vol, 13 % for TDL, 0 % for MSL, 11 % for DSC) and spine (by 26 % for DSN, and 14 % for DSD) extent than those in visual regions. Individual spiny neuron tracings are depicted for the visual cortex in Fig. 5, and for the motor cortex in Fig. 6. Aspiny neuron tracings are provided in Fig. 7, and Sholl analyses for all neuron types are illustrated in Fig. 8. Below, we provide more detailed descriptions of spiny and aspiny neuron types based on examination of all Golgi-stained sections as well as the quantified neurons themselves.

Spiny neurons

Typical pyramidal neurons ($n = 143$; Figs. 3a, d, 4e, 5A–J, 6A–H), considered "typical" because they resemble those in anthropoid primate and murid rodent models, were the

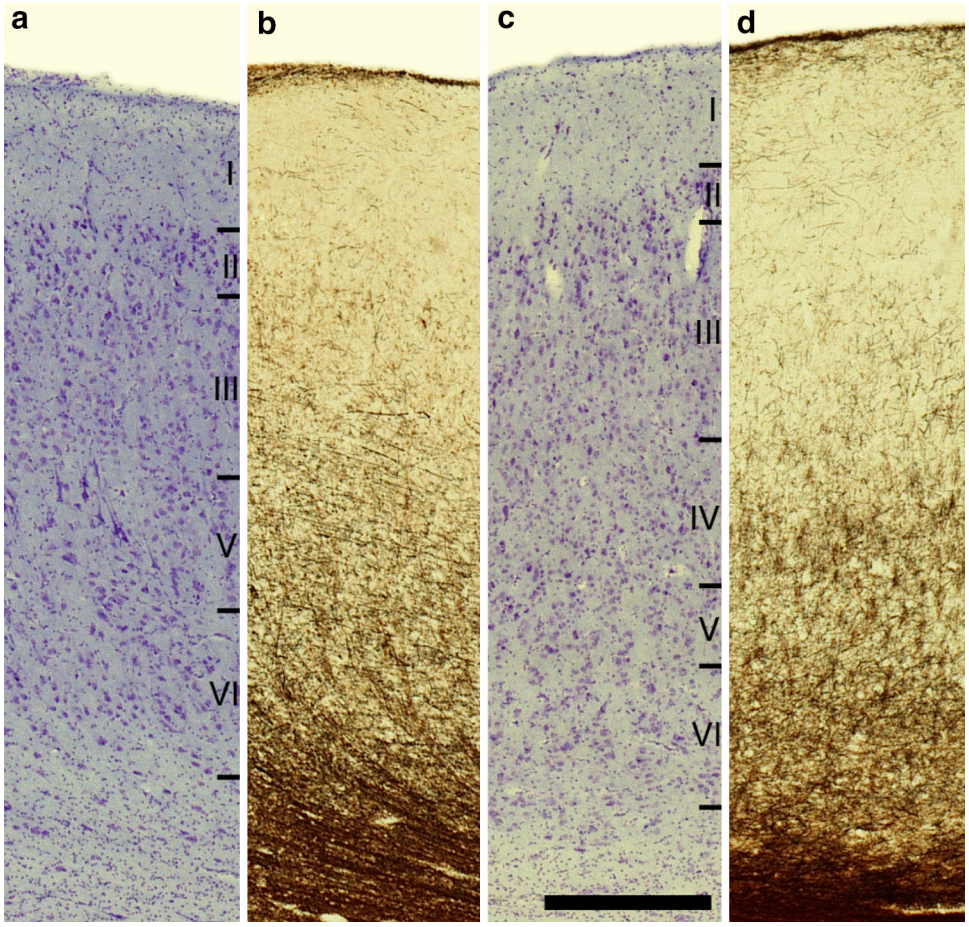

Fig. 2 Photomicrographs of Nissl (**a**, **c**) and myelin (**b**, **d**) stained sections through the primary motor (**a**, **b**) and primary visual (**c**, **d**) cortices with the layers labeled. Note the large pyramidal neurons in layer V of the primary motor cortex (**a**) and the lack of layer IV in this cortical area. Layer IV appears to be present in the primary visual cortex (**c**) as does the stria of Gennari in the lower half of layer IV (**d**). *Scale bar* 500 μm

Table 1 Laminar and cortical thickness (in μm, mean ± SD) in giraffe cortex

	Motor	Visual
Layer I	379 ± 17	255 ± 19
Layer II	180 ± 33	134 ± 12
Layer III	516 ± 59	293 ± 24
Layer IV	–	180 ± 19
Layer V	157 ± 24	176 ± 16
Layer VI	359 ± 57	287 ± 15
Total cortical thickness	1,591 ± 90	1,325 ± 36

most prominent neuron type traced in both primary motor ($n = 78$) and visual cortices ($n = 65$). Somata, located at an average depth of ~1,000 μm (Table 2), were usually triangular with a single, sometimes bifurcating apical dendrite and an average of 4.93 ± 1.53 primary basilar dendrites that radiated in all directions to form a circular skirt. Superficial pyramidal neurons tended to have more widely divergent apical dendrites whereas deeper pyramidal neurons exhibited longer apical dendrites with fewer bifurcations. All dendrites were relatively spiny (DSD = 0.83, Table 2). Sholl analysis indicated that pyramidal neurons exhibited an intersection pattern similar to, but slightly less complex than the larger magnopyramidal and gigantopyramidal neurons described below (Fig. 8c).

Magnopyramidal neurons ($n = 10$; Figs. 5R, S, 6P, Q), located in both cortical regions at an average depth of ~1,400 μm (Table 2), were morphologically similar to pyramidal neurons but were much larger in terms of Vol (by 122 %), TDL (by 17 %), MSL (by 15 %) and soma size (by 102 %; Table 2). They displayed an average of 7.6 ± 3.13 primary basilar dendrites per neuron. The dendrites of magnopyramidal neurons were marginally less spiny (DSD = 0.76) than those of pyramidal neurons. Sholl analysis revealed a higher density of basilar dendritic intersections for magnopyramidal neurons than for pyramidal neurons (Fig. 8b).

Gigantopyramidal neurons ($n = 6$, Figs. 4a, g, 6K, L), located only in the motor cortex, were the largest neurons examined, particularly in terms of Vol (113 % > magnopyramidal neurons, and 375 % > pyramidal neurons), but also in terms of TDL (47 % > magnopyramidal neurons, and 72 % > pyramidal neurons), MSL (10 % > magnopyramidal neurons, and 26 % > pyramidal neurons), and soma size (80 % > magnopyramidal neurons, and 265 % > pyramidal neurons; Table 2). The fusiform somata, located at an average depth ~1,500 μm, typically extended a single apical dendrite, although one gigantopyramidal neuron exhibited a fork-like soma (Ngowyang 1932) with two, parallel, ascending apical dendrites (Figs. 4g, 6K). The basilar dendrites of gigantopyramidal neurons resembled the perisomatic, circumferential dendrites of Betz cells described by Scheibel and Scheibel (1978a) and were the highest in number as compared to all other neuron types (an average of 13 ± 5.5 primary dendritic segments/neuron). Dendrites were highly spiny, with a DSD (0.91) equal to that of extraverted neurons (Table 2). Sholl analyses indicated that gigantopyramidal neurons, despite their relatively short basilar dendrites, were characterized by a higher density of basilar dendritic intersections than any other neuron types (Fig. 8a).

Extraverted neurons ($n = 35$, Figs. 3e, 4d, 5K–M, 6M–O), located in both cortical regions at an average depth ~600 μm (Table 2), were the most superficial neuron type. These were roughly comparable to pyramidal neurons in terms of quantitative dendritic measurements, although basilar dendritic number (3.89 ± 1.7 primary dendritic segments/neuron) and extent were lower than in pyramidal neurons. This is the only neuron type where apical dendritic length was greater than basilar dendritic length (by 5.27 %). Somata ranged from triangular to globular in shape with apical bifurcations at or immediately above the soma such that there were two individual, ascending branches. DSD (0.91) was equal to that of gigantopyramidal neurons (Table 2). Sholl analyses indicated that apical dendrites had a higher density of intersections than did other neuron types, although basilar dendritic intersections were the lowest density among all other spiny neuron types (Fig. 8d).

Horizontal pyramidal neurons ($n = 17$, Figs. 3i, 5P, Q, 6I, J), located in both cortical regions at an average depth of ~1,300 μm, exhibited an apical dendrite that extended laterally or obliquely (<45°) from a triangular soma. Most of these (15 of 17) were located deep in the sulcus, with the rest located in intermediate sulcal regions. Basilar dendrites (4.41 ± 1.94 primary dendritic segments/neuron) radiated from the soma in all directions and tended to be quite long relative to basilar dendrites in other spiny neurons. Overall, horizontal pyramidal dendrites were moderately spiny (DSD = 0.67; Table 2). Sholl analyses revealed a pattern similar to that observed in pyramidal neurons (Fig. 8e). Axons, when visualized, initially extended towards the basilar dendrites but typically turned to travel parallel to the apical dendrite.

Crab-like neurons ($n = 4$, Figs. 3c, 5N, O), traced only in the visual cortex, had oval or rounded somata (at an average depth of ~1,100 μm) from which dendrites (4.5 ± 0.58 primary dendritic segments/neuron) radiated symmetrically from opposite ends. These horizontally, bitufted neurons (Jacobs et al. 2011) were the smallest of all spiny neuron types, with the lowest spine values as well (Table 2). Sholl analyses indicated that crab-like neurons had the lowest density of basilar dendritic intersections and shortest dendritic length of all spiny neurons (Fig. 8f).

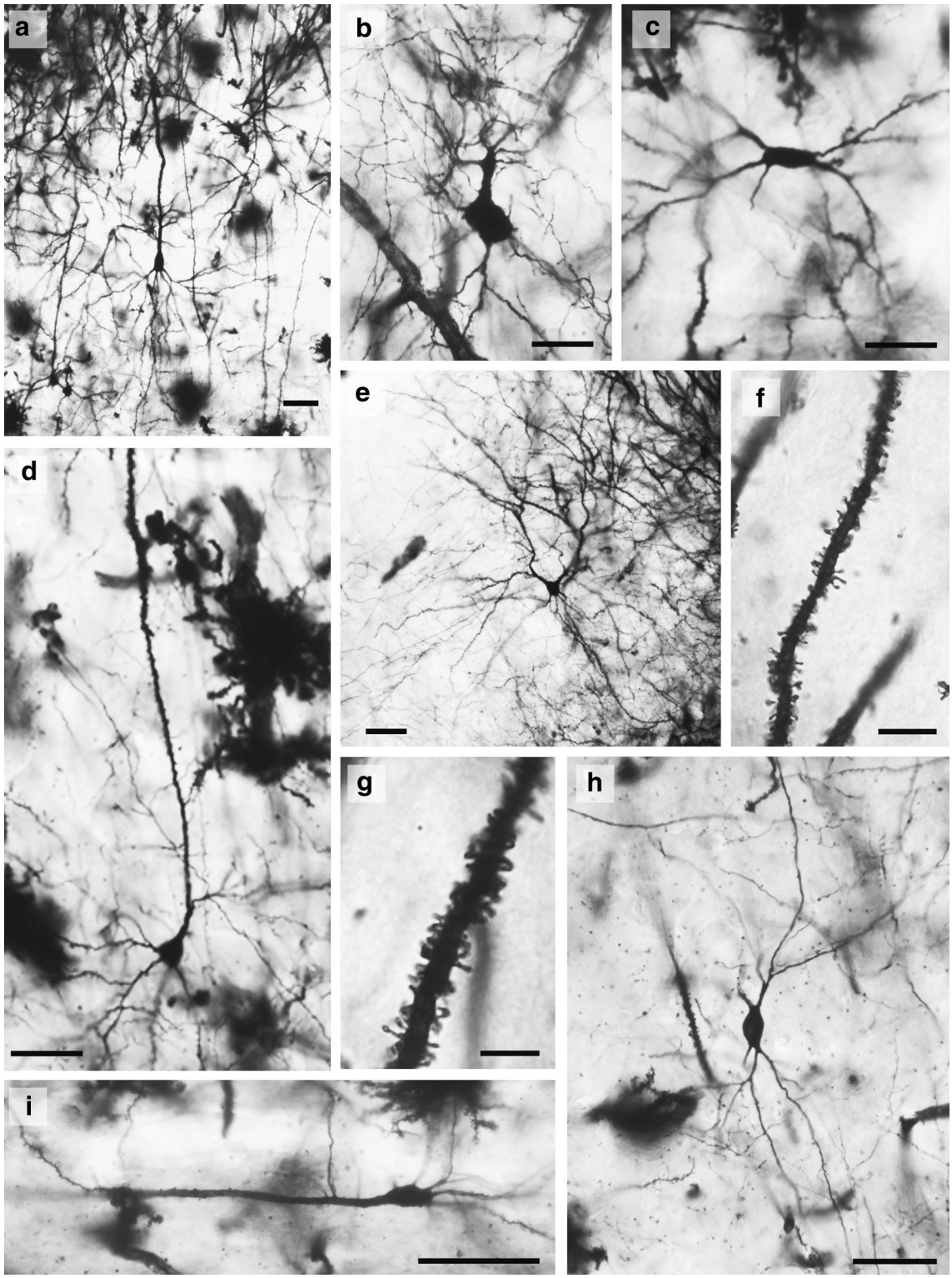

Fig. 3 Photomicrographs of Golgi-stained neurons in the primary visual cortex: pyramidal neurons (**a**, **d**); neurogliaform neuron (**b**); crab-like neuron (**c**); extraverted neuron (**e**); higher magnification of basilar (**f**) and apical (**g**) dendritic segments; aspiny neuron (**h**); horizontal pyramidal neuron (**i**, see also Fig. 5P). *Scale bar* (**a**, **c**–**e**, **h**, **i**) 100 μm. *Scale bar* (**b**, **f**, **g**) 50 μm

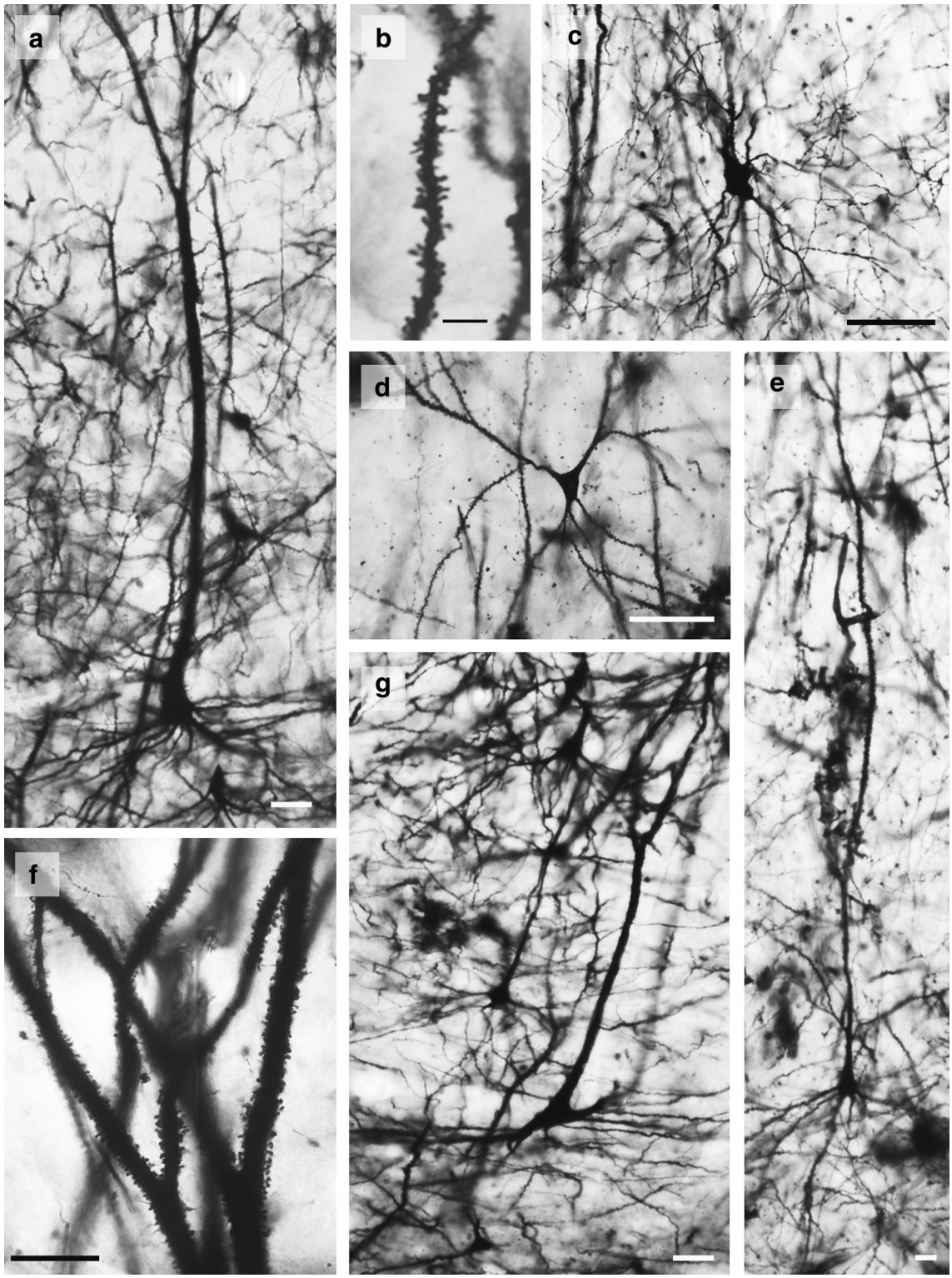

Fig. 4 Photomicrographs of Golgi-stained neurons in the primary motor cortex: gigantopyramidal neurons (**a**, see also Fig. 6L; **g**, see also Fig. 6K); higher magnification of basilar (**b**) and apical (**f**) dendritic segments; neurogliaform neuron (**c**); extraverted neuron (**d**, see also Fig. 6O); pyramidal neuron (**e**). *Scale bar* (**a**, **c**–**f**) 100 μm. *Scale bar* (**b**, **g**) 50 μm

Table 2 Summary statistics (mean ± SEM) for each type of giraffe neuron quantified in primary motor and visual cortices

Type	*n*	Vol	TDL	MSL	DSC	DSN	DSD	SoSize	SoDepth
Spiny									
Motor									
Gigantopyramidal	6	68,547 ± 33,632	7,882 ± 2,201	101 ± 9	78 ± 22	7,232 ± 2,270	0.91 ± 0.10	1,184 ± 246	1,494 ± 190
Extraverted	19	19,298 ± 7,461	4,566 ± 1,149	79 ± 8	58 ± 14	4,264 ± 947	0.94 ± 0.10	374 ± 112	616 ± 181
Horizontal	7	17,645 ± 5,503	4,649 ± 2,149	72 ± 16	63 ± 16	3,307 ± 1,406	0.73 ± 0.13	432 ± 110	1,177 ± 412
Magnopyramidal	4	34,896 ± 8,348	5,662 ± 1,198	93 ± 9	61 ± 12	4,790 ± 1,005	0.86 ± 0.15	634 ± 77	1,481 ± 275
Pyramidal	78	16,659 ± 7,002	4,809 ± 1,296	80 ± 12	61 ± 13	4,119 ± 1,263	0.86 ± 0.17	349 ± 106	968 ± 421
Visual									
Crab-like	4	4,923 ± 1,111	2,711 ± 596	64 ± 5	43 ± 8	1,192 ± 310	0.46 ± 0.16	207 ± 21	1,132 ± 121
Extraverted	16	12,560 ± 4,689	4,441 ± 815	74 ± 13	61 ± 12	3,953 ± 1,128	0.88 ± 0.14	346 ± 113	625 ± 225
Horizontal	10	9,731 ± 4,391	3,343 ± 704	79 ± 14	43 ± 8	2,155 ± 878	0.63 ± 0.15	304 ± 103	1,432 ± 565
Magnopyramidal	6	30,412 ± 14,413	5,186 ± 1,295	91 ± 13	57 ± 10	3,518 ± 904	0.70 ± 0.19	671 ± 339	1,385 ± 358
Pyramidal	65	11,889 ± 5,381	4,295 ± 1,149	79 ± 12	54 ± 14	3,435 ± 1,384	0.79 ± 0.18	293 ± 71	1,012 ± 418
Aspiny									
Motor									
Aspiny	5	6,360 ± 4,302	2,538 ± 768	93 ± 24	28 ± 6	0	0	282 ± 66	1,262 ± 420
Neuroglial	6	4,677 ± 1,636	4,193 ± 1,211	43 ± 18	103 ± 21	0	0	267 ± 93	1,363 ± 321
Visual									
Aspiny	15	6,038 ± 3,221	2,815 ± 1,180	70 ± 18	41 ± 13	0	0	288 ± 60	1,003 ± 301
Neuroglial	3	5,248 ± 1,088	4,660 ± 945	38 ± 5	126 ± 38	0	0	263 ± 46	1,157 ± 60

n number of neurons of a given type traced in each cortical region, *Vol* volume (in μm^3) of all dendritic branches in a neuron, *TDL* total dendritic length in μm (i.e., the summed length of all dendritic branches in a neuron), *MSL* mean segment length in μm (i.e., average length of individual dendritic branches), *DSC* dendritic segment count (i.e., the number of dendritic segments per neuron), *DSN* dendritic spine number (i.e., the total number of spines per neuron), *DSD* dendritic spine density (i.e., the number of spines per μm of dendritic length), *SoSize* neuronal soma size in μm^2, *SoDepth* depth of the neuronal soma in μm from the pial surface

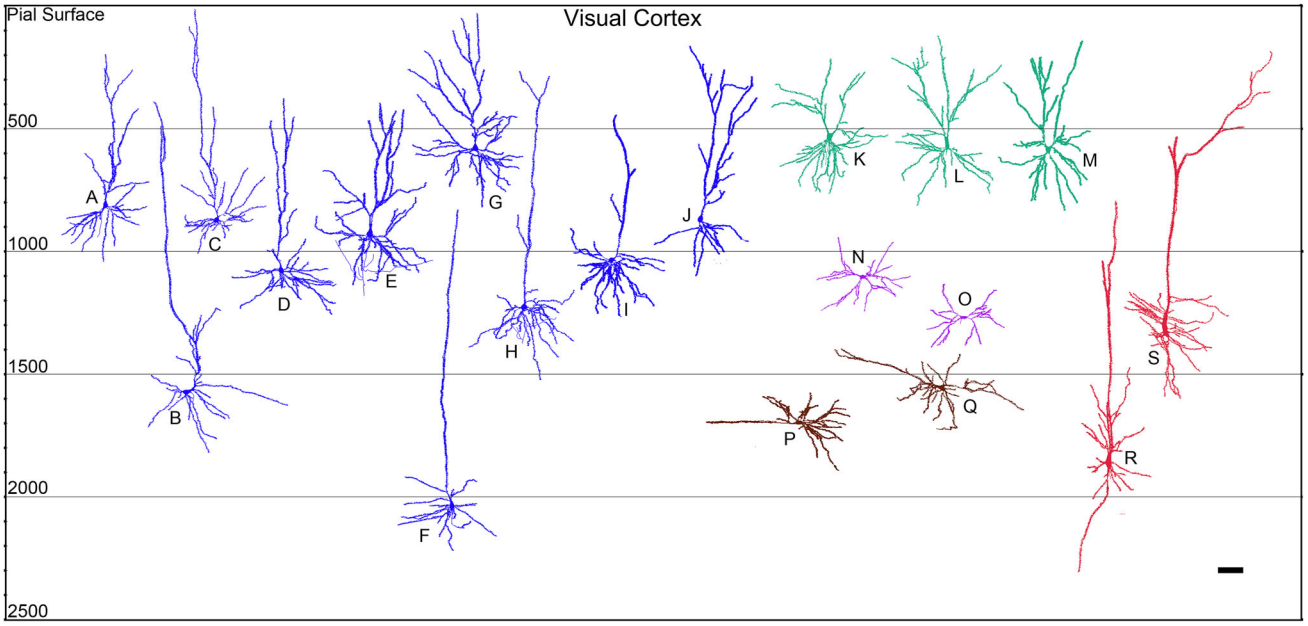

Fig. 5 Sample neurolucida tracings of spiny neurons in the giraffe primary visual cortex indicating relative soma depth from the pial surface (in μm): pyramidal neurons (*A*–*J*); extraverted neurons (*K*–*M*); crab-like neurons (*N*, *O*); horizontal pyramidal neurons (*P*, *Q*); magnopyramidal neurons (*R*, *S*). *Scale bar* 100 μm

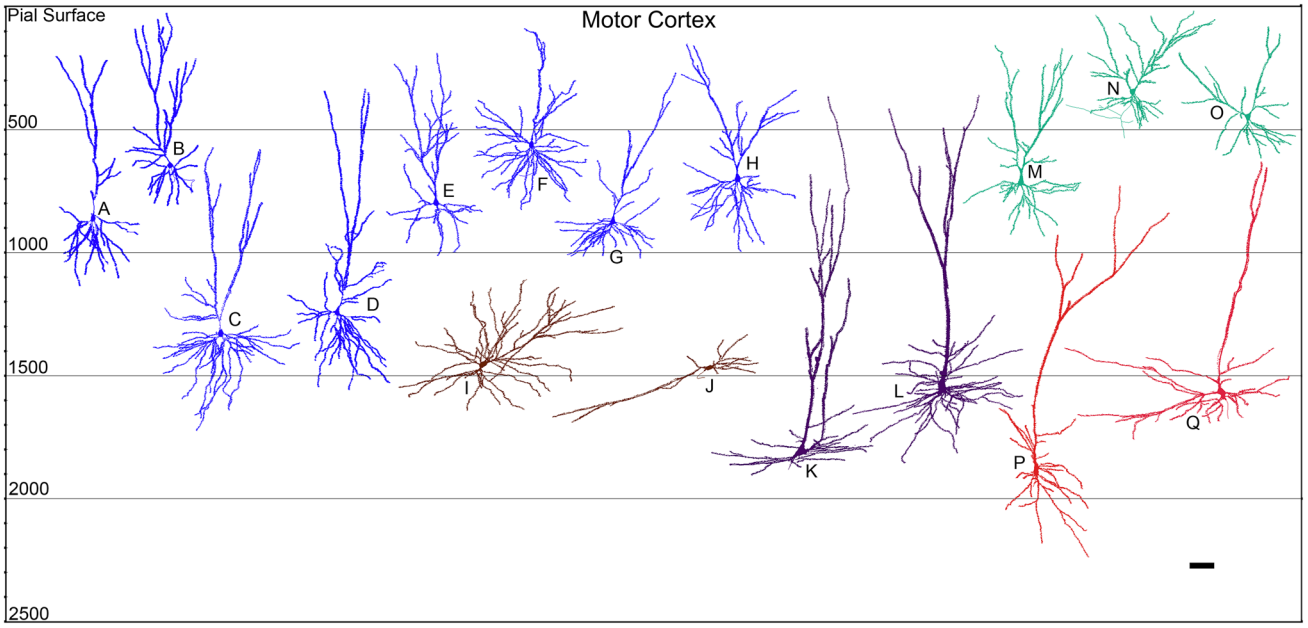

Fig. 6 Sample neurolucida tracings of spiny neurons in the giraffe primary motor cortex indicating relative soma depth from the pial surface (in μm): pyramidal neurons (*A*–*H*); horizontal pyramidal neurons (*I*, *J*); gigantopyramidal neurons (*K*, *L*); extraverted neurons (*M*–*O*); magnopyramidal neurons (*P*, *Q*). *Scale bar* 100 μm

Aspiny neurons

Aspiny neurons ($n = 20$, Figs. 3h, 7A–E, 7I–L) were distributed at various depths (averaging ~1,700 μm; Table 2) in both cortical regions. They were characterized by rounded somata with straight, minimally branching dendrites (8.85 ± 4.88 primary dendritic segments/neuron) that extended up to 600 μm. Two subtypes of aspiny neurons were noted: multipolar neurons, which possessed multiple dendrites that extended radially in all

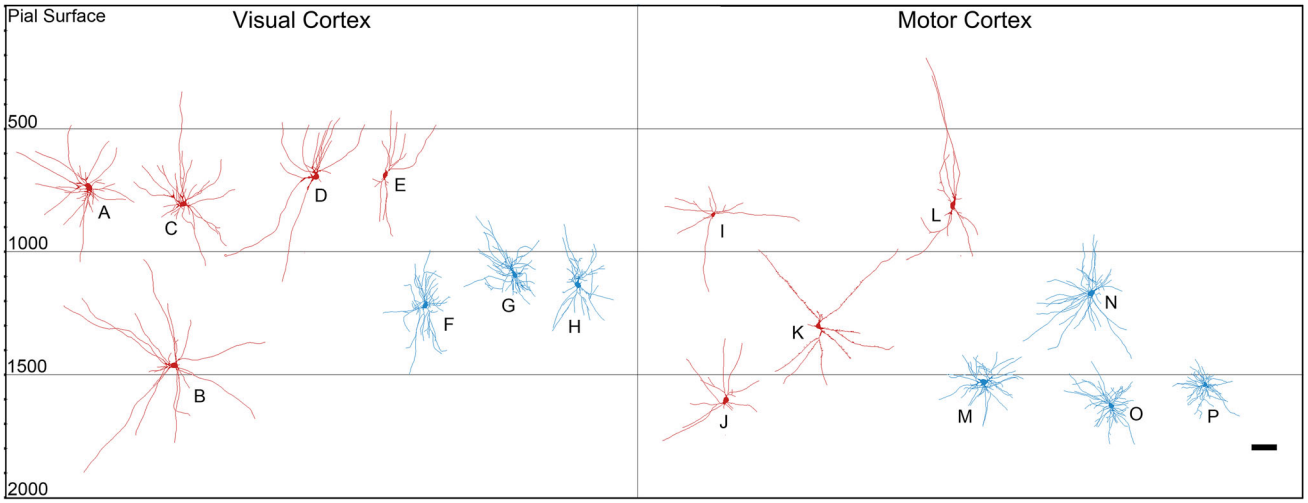

Fig. 7 Sample neurolucida tracings of aspiny neurons in giraffe primary visual (*A–H*) and motor cortices (*I–P*) indicating relative soma depth from the pial surface (in μm): multipolar aspiny neurons (*A–D*; *I–K*); bitufted aspiny neurons (*E*, **l**); neurogliaform neurons (*F–H*; *M–P*). *Scale bar* 100 μm

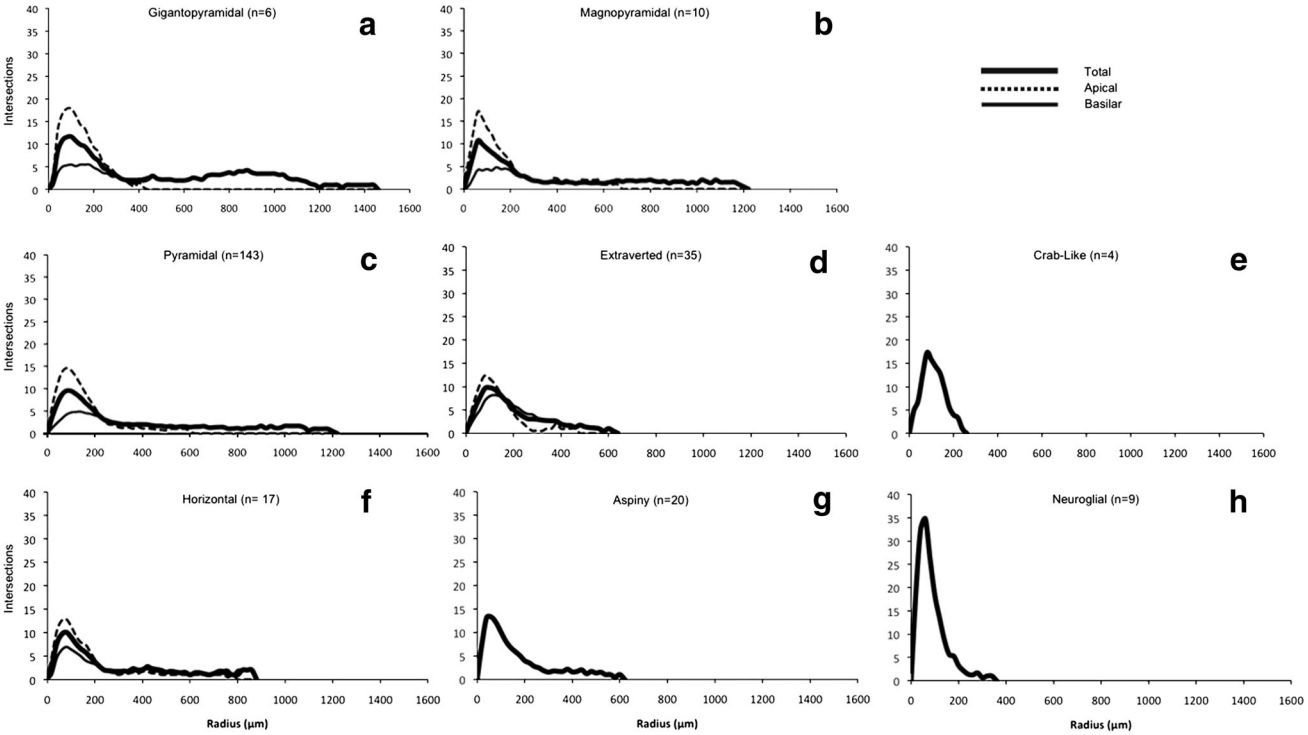

Fig. 8 Sholl analyses of eight cell types indicating relative basilar, apical, and total dendritic complexity of branching patterns. Dendritic intersections were quantified at 20-μm intervals using concentric rings. Neurons **a–f** were spiny and neurons **g** and **h** were aspiny. **a–c** had relatively long apical dendrites whereas **d**, **e** had shorter apical dendrites. For all cells, relative dendritic intersections peaked before 200 μm. Apical dendrites either extended much further than the basilar dendrites (**a–c**) or were of similar length (**d**, **e**)

directions from the soma (Figs. 7A–D, I–K), and bitufted neurons (Figs. 3h, 7E, L), which exhibited two dendritic tufts that extended from opposite poles of the soma. Sholl analyses indicated that aspiny neurons had the lowest density of dendritic intersections of all neuron types (Fig. 8g).

Neurogliaform neurons ($n = 9$, Figs. 3b, 4c, 7F–H, M–P), also referred to as "spiderweb" cells (Ramón y Cajal

1922) or "clewed" cells (Valverde 1971), were traced throughout the cortical layers (average depth ~1,300 μm; Table 2) and exhibited a dense dendritic plexus that arose in all directions from a rounded soma. Dendrites (9.44 ± 2.13 primary dendritic segments/neuron) extended an average of 400 μm with most bifurcations occurring close to the soma. DSC for neurogliaform neurons was 189 % greater than DSC for other aspiny neurons (Table 2). Accordingly, Sholl analyses revealed the highest density of dendritic intersections close to the soma, with nearly twice as many intersections as any other neuron type (Fig. 8h).

Regional dendritic variation

Inferential analyses of regional differences were focused only on pyramidal neurons. Review of cluster analysis indicated considerable and varying skew and kurtosis in the distributions of pyramidal dendritic measures between the two Brains (G1 and G3) and two Regions (Motor and

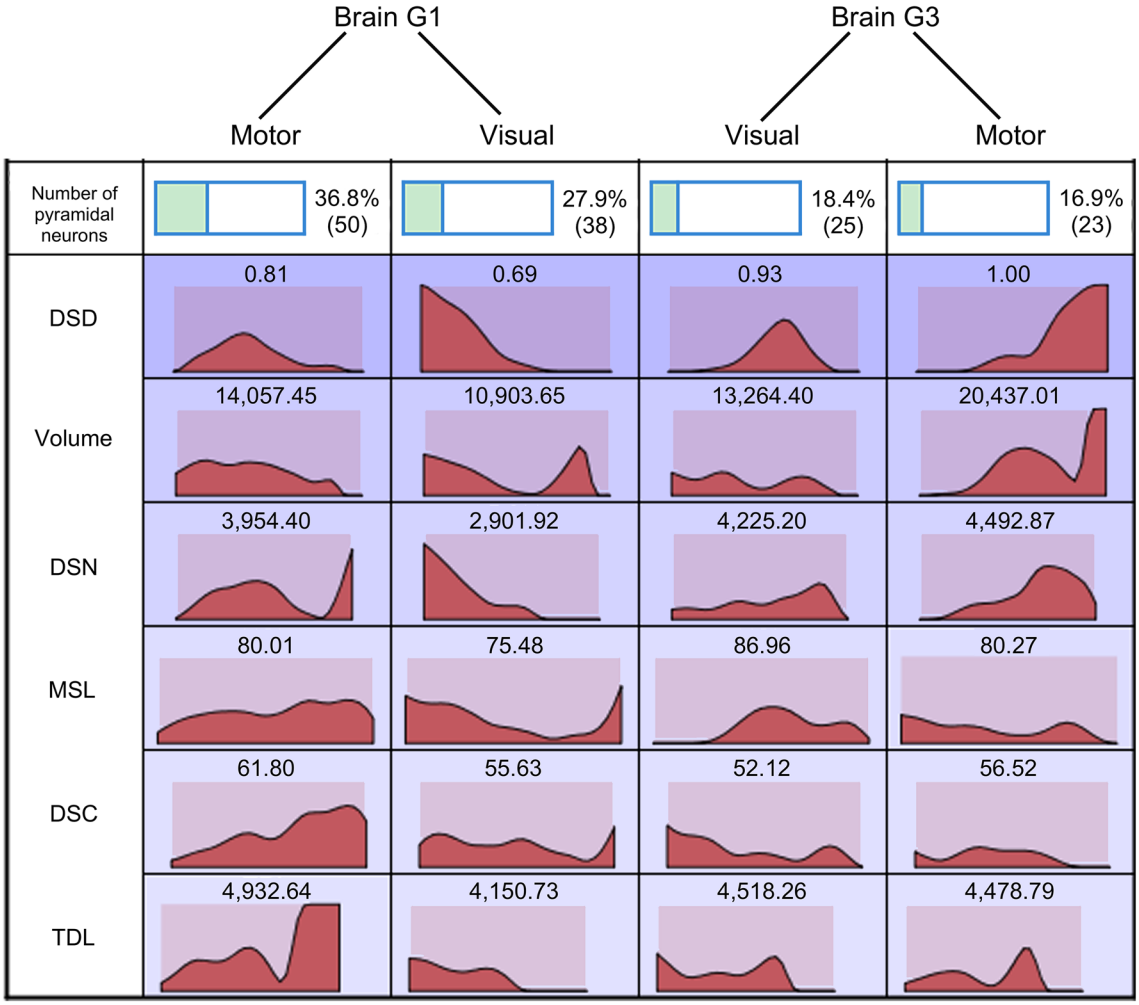

Fig. 9 A cluster analysis characterizing the six dendritic measures of pyramidal neurons ($n = 136$) for Brains G1 ($n = 88$) and G3 ($n = 48$) and the visual and motor Regions within those Brains. Because only a small number of pyramidal neurons ($n = 7$) were traced in Brain G2, it was excluded from the cluster analysis. Four clusters emerged, one for each combination of Brains G1 and G3 and their two Regions. The first row of the figure provides the number and percentages of pyramidal neurons falling within each Region of each Brain (e.g., 50 neurons of the 136 total were from the motor region of Brain G1, or 36.8 %). Subsequent rows indicate the distributions of each dendritic measure (e.g., DSD, Volume, DSN, MSL, DSC, TDL—see Table 2 for abbreviations) for each cluster, with the mean of these measures above each histogram for that cell (e.g., $\text{Mean}_{\text{DSD}} = 0.81$ for the Motor Region of G1). The dependent measures are arranged in relative order of importance from top to bottom. This qualitative depiction of the data reveals that the distributions across Visual and Motor Regions within Brain vary considerably, even for the same dependent measure. For example, although DSD looks normally distributed for the Visual region within Brain G3, comparing across brains on DSD reveals considerable skew and kurtosis in the distributions shown in the corresponding cells. See text for further details

Visual, Fig. 9). This heterogeneity underscored why conventional statistical tests were inappropriate for additional quantitative analyses. Decision trees results were inconsistent, with significant Brain and asymmetric Region effects for DSD on Brains G2 and G3 versus G1, and significant Brain and asymmetric Region effects for Vol on Brains G2 and G3 versus G1. These distributional results motivated the use of a GENLIN model with a normal distribution and an identity link function. Four of the dependent variable models had a significant Brain main effect and three had a significant Region within Brain effect, but only the model for DSD fit the data (Table 3), indicating a significant difference between Regions for DSD (motor cortex > visual cortex) but also underscoring the extensive variability within the data.

Discussion

Grossly, the giraffe brain appears to be roughly the same size as the horse (*Equus caballus*) brain ($Mean_{weight} = 599$ g; Cozzi et al. 2014). Cytoarchitectonically, insofar as giraffe visual cortex exhibits a layer IV, it may differ slightly from cetartiodactyls such as the pygmy hippopotamus (Butti et al. 2011) and several cetacean species (Morgane et al. 1988; Glezer and Morgane 1990; Hof et al. 2005; Hof and Van der Gucht 2007; Oelschläger 2008; Butti et al. 2014a), which display an agranular cerebral cortex lacking in a detectable layer IV across all regions. Futher, the cytoarchitecture of the giraffe cerebral cortex contrasts with that of primate primary visual cortex, which exhibits an extraordinarily expanded layer IV that is divided into multiple sublaminae and a primary motor cortex characterized by a lower cell packing density, increased overall cortical thickness, and a predominance of large pyramidal neurons in layer V (Brodmann 1909). Before firm conclusions can be reached, however, more in depth examination of laminar differentiation using molecular signatures (e.g., the *RORB* gene) is warranted to determine the exact extent of layer IV in the giraffe as well as other cetartiodactyls (Zeng et al. 2012).

In terms of neuronal morphology, giraffe neurons appear similar to those documented in other cetartiodactyls, particularly in ungulates (Barasa 1960) and cetaceans (Butti et al. 2014b). However, there are also some important differences, both in terms of neuron types and specific morphologies. Giraffe neocortex exhibits an array of complex spiny neurons with singular or narrowly bifurcating apical dendrites contributing to a largely vertical columnar organization similar to typical rodent/primate cortical organization (Mountcastle 1997; Innocenti and Vercelli 2010). Quantitatively, although spiny neurons in the motor cortex tended to be more complex than those in the visual cortex, inferential analysis of pyramidal neurons suggested that only DSD measures indicated a consistent significant regional difference in favor of the primary motor region. Further interpretation of these results first requires consideration of several methodological issues.

Methodological considerations

Many of the general constraints that apply to Golgi-stained human materials also apply here, and have been outlined in more detail elsewhere (Jacobs and Scheibel 2002; Jacobs et al. 2011): (1) lack of historical information on the subjects (Jacobs et al. 1993); (2) a small sample size in terms

Table 3 Evaluation of effects in initial exploratory models

Dependent variable[a]	Overall model compared to intercept only model[b]	Model fit Pearson χ^2 [c]	Model fit conclusion	Intercept Wald χ^2	Brain main effect Wald χ^2	Block within Brain Wald χ^2
DSC	n.s.	χ^2 (137) = 25,940.9, $p \leq 0.000$	Model does not fit the data	χ^2 (1) = 775.5, $p \leq 0.000$	n.s.	n.s.
DSD	χ^2 (5) = 64.5, $p \leq 0.000$	χ^2 (137) = 2.9, $p > 0.05$	Model fits the data	χ^2 (1) = 5,207.0, $p \leq 0.000$	χ^2 (2) = 58.4, $p \leq 0.000$	χ^2 (3) = 19.7, $p \leq 0.000$
DSN	χ^2 (5) = 28.7, $p \leq 0.000$	χ^2 (137) = 2.1E8, $p \leq 0.000$	Model does not fit the data	χ^2 (1) = 662.8, $p \leq 0.000$	χ^2 (2) = 15.6, $p \leq 0.000$	χ^2 (3) = 20.8, $p \leq 0.000$
MSL	χ^2 (5) = 16.7, $p \leq 0.000$	χ^2 (137) = 19,160.3 $p \leq 0.000$	Model does not fit the data	χ^2 (1) = 7,525.9, $p \leq 0.000$	χ^2 (2) = 19.1, $p \leq 0.000$	n.s.
TDL	n.s.	χ^2 (137) = 2.1E8, $p \leq 0.000$	Model does not fit the data	χ^2 (1) = 811.2, $p \leq 0.000$	n.s.	n.s.
Vol	χ^2 (5) = 51.2, $p \leq 0.000$	χ^2 (137) = 4.5E9, $p \leq 0.000$	Model does not fit the data	χ^2 (1) = 480.2, $p \leq 0.000$	χ^2 (2) = 26.2, $p \leq 0.000$	χ^2 (3) = 35.2, $p \leq 0.000$

[a] See Table 2 for abbreviations

[b] A significant result indicates that we can reject H_0 that the model is no better than a model with just the intercept term

[c] A significant result indicates that we can reject H_0 that the model fits the data (adequately captures sources of variability)

of subjects, with an uneven, limited sampling of neurons among these subjects (Jacobs and Scheibel 1993); (3) inherent issues with fixation and Golgi impregnations (Williams et al. 1978; Braak and Braak 1985) and attenuated dendritic measures because of section thickness (Jacobs et al. 1997); (4) underestimation of spines in light microscopy (Horner and Arbuthnott 1991); and (5) problems of neuronal classification (Germroth et al. 1989; Masland 2004; Bota and Swanson 2007; DeFelipe et al. 2013) based solely on somatodendritic architecture (Nelson et al. 2006; The Petilla Interneuron Nomenclature Group et al. 2008), particularly when biased by an essentially Euarchontoglires-centric nomenclature in the literature (Manger et al. 2008).

It should be noted that comparative neuroanatomical statements based on Golgi impregnations are inherently constrained because one cannot definitively determine the presence or absence of cell types. As such, one can only make general observations about the relative number or distribution of cell types either within or across species. Currently, although cytoarchitectural studies have delineated the giraffe primary motor cortex (Badlangana et al. 2007b), the lack of functional information about regions sampled in the present study preclude firm morphological-functional correlations in these regions, as has been done in primates (Elston and Rosa 1998a, b; Jacobs et al. 2001). Nevertheless, two factors suggest the correct identification of these two cortical regions in the current sample: (1) the presence of gigantopyramidal neurons in the primary motor cortex that resemble Betz cells (Betz 1874), and (2) the presence of magnopyramidal neurons in the primary visual cortex that resemble the solitary gigantopyramidal cells of Meynert (Chan-Palay et al. 1974). As such, the present neuromorphological descriptions should be relatively accurate depictions of primary motor and visual cortices in the giraffe.

Spiny neurons

Spiny neurons in the giraffe ranged from those that were pyramidal-like (e.g., pyramidal, magnopyramidal, gigantopyramidal, and extraverted neurons) to those that were more atypical in orientation (e.g., horizontal pyramidal neurons) or structure (e.g., crab-like neurons). Beyond the results highlighted below, specific comparisons of neuronal types for each dendritic measure in different cortical regions across species (e.g., giraffe, bottlenose dolphin, minke whale, and humpback whale) can be made by comparing Table 2 of the present paper with Table 1 in Butti et al. (2014b). The most frequently traced neuron in the giraffe was the pyramidal neuron, which usually exhibited either a single apical shaft with associated apical oblique branches similar to what typifies primate pyramidal neurons (de Lima et al. 1990), or an acutely bifurcating apical dendrite similar to what is common in some ungulates, the pygmy hippopotamus, and cetaceans. Specifically, within ungulates, giraffe pyramidal neurons appear morphologically similar to those of the pig and sheep, but differ considerably from those in the horse and cow (Barasa 1960; Ferrer et al. 1986b), both of which exhibit more widely bifurcating, V-shaped apical dendrites that resemble those found in the elephant (Jacobs et al. 2011). Giraffe pyramidal neurons tend to resemble the typical pyramidal neurons (i.e., possessing a prominent apical dendrite that may bifurcate some distance from the soma) rather than the multiapical pyramidal neurons found in the pygmy hippopotamus (Butti et al. 2014a). Moreover, giraffe pyramidal neurons appear qualitatively similar to those in cetaceans, particularly in terms of apical dendritic morphology (Garey et al. 1985; Ferrer and Perera 1988; Butti et al. 2014b). Nevertheless, one pyramidal neuron variant that is prominent in cetaceans does not appear in the giraffe cortex: tri-tufted pyramidal neurons, which exhibit three primary dendritic branches, namely an apical and two basilar dendrites at 90° angles to each other (Butti et al. 2014b). At this point, it remains unclear whether this particular variant does not exist in the giraffe or whether they simply did not stain. The quantitative attributes of pyramidal neurons are discussed below.

Morphologically similar to giraffe pyramidal neurons are the much larger magnopyramidal neurons, which were found exclusively in deeper cortical layers. These neurons are common in laurasiatherians, having been documented in classical language areas in humans (Braak 1978; Hayes and Lewis 1995), and in primate visual cortex as the solitary cells of Meynert (Meynert 1867; le Gros Clark 1942; Hof et al. 2000). In the giraffe, magnopyramidal neurons in visual cortex resemble Meynert neurons in the primate, both in terms of morphology and in terms of their relatively equal spacing ($\sim$400 μm between neurons; Chan-Palay et al. 1974). This spacing is slightly less than the $\sim$500 μm noted in the humpback whale (Butti et al. 2014b). Quantitatively, magnopyramidal neurons in the giraffe were similar in both Vol and TDL to those documented in the minke whale (Butti et al. 2014b), making them larger than those observed in the dolphin (by 82 % for Vol, and by 23 % for TDL), but smaller than those observed in the humpback whale (by 72 % for Vol, and by 66 % for TDL). Functionally, to the extent that these neurons evolved in a species that migrated into open territory, where increased visual dependence is necessary for predator detection and survival, their presence in the visual cortex of the current study may underscore the importance of visual abilities in giraffes, especially considering that somatic volume of these neurons has been demonstrated to correlate with habitat type in primates (Sherwood et al. 2003; Coimbra

et al. 2013). Within ungulates, the giraffe magnopyramidal neurons clearly resemble pig gigantopyramidal neurons (Barasa 1960) as well as the magnocellular neurons observed in layer V of the putative motor cortex in the pygmy hippopotamus (Butti et al. 2014a); however, both pig and pygmy hippopotamus magnopyramidal neurons have apical dendrites that tend to bifurcate further away from the soma than in the giraffe.

Substantially larger than the magnopyramidal neurons were the spine-rich gigantopyramidal neurons found in the deeper layers of giraffe motor cortex. Although the term "Betz cell" has usually been reserved for gigantopyramidal neurons in layer Vb of human (and, by extension primate) motor cortex (Braak and Braak 1976; Rivara et al. 2003; Sherwood et al. 2003), Betz (1874) himself noted smaller variants in dogs, and others have applied the term to gigantopyramidal neurons in non-primate species (cats: Crawford and Curtis 1966; Kaiserman-Abramof and Peters 1972; rats: Phillis and Limacher 1974). However, in the absence of information about the pigmentoarchitecture, specific connectivity, and functional attributes, it is impossible to determine if giraffe gigantopyramidal neurons meet the defining criteria for Betz cells. In the present study, these neurons had a soma size ($\sim$1,200 μm^2) comparable to human Betz neurons (Sasaki and Iwata 2001), but were notably larger than those observed by Badlangana et al. (2007b) in giraffe motor cortex based on Nissl staining ($\sim$600 μm^2). Distinguishing magnopyramidal from gigantopyramidal neurons based on soma size is difficult (Walshe 1942), especially because their dimensions are known to overlap (von Bonin 1938; Rivara et al. 2003). As such, the gigantopyramidal neurons noted in cresyl violet stains by Badlangana et al. (2007b) may be the same as the magnopyramidal neurons quantified in the present Golgi study (soma size = $\sim$656 μm^2), or they may simply be smaller variants of gigantopyramidal neurons. Regardless, both the extensive dendritic Vol and the distinctive presence of a large number (i.e., $\sim$13) of circumferential dendrites per neuron, which falls within the range (i.e., 7–15) for Betz cells (Betz 1874), indicate morphological similarity between the traced gigantopyramidal neurons in the giraffe and human Betz cells. Whether these similarities extend to the functional realm remains unclear.

Much smaller in scale is a neuronal type found across many species, the extraverted neuron, which has been documented in (semi-) aquatic (cetaceans: Kraus and Pilleri 1969a, b; Ferrer and Perera 1988; Glezer and Morgane 1990; Hof and Van der Gucht 2007; pygmy hippopotamus: Butti et al. 2014a) and terrestrial species (opossums, bats, hedgehogs, monkeys: Sanides and Sanides 1972; quokkas: Tyler et al. 1998; giant elephant shrews and anteaters: Sherwood et al. 2009; elephants: Jacobs et al. 2011). Its appearance as the second most prominent neuronal type traced in the giraffe motor and visual cortices is therefore not surprising, and is consistent with our own observations in cetaceans (Butti et al. 2014b). Overall morphology was typical of extraverted neurons described previously, with a relatively wide apical dendritic array that was more extensive than the more limited basilar dendritic system (Sanides and Sanides 1972). Quantitatively, extraverted neurons in the giraffe were larger in both Vol and TDL than those documented in the dolphin (by 182 % for Vol, and by 170 % for TDL) and minke whale (by 46 % for Vol, and by 100 % for TDL), but similar to those observed in the humpback whale (Butti et al. 2014b). Although originally believed to represent a more primitive type of cortical neuron (Sanides and Sanides 1972; Morgane et al. 1985), it seems more likely that extraverted neurons are common in those species (e.g., giraffe, cetaceans, pygmy hippopotamus, and African elephant) that possess predominantly agranular cortices (Jacobs et al. 2011; Butti et al. 2014a, b). Functionally, the wide apical bouquet of extraverted neurons in these species facilitates communication within superficial layers, where many thalamocortical afferents tend to synapse (Sanides and Sanides 1972; Ferrer 1987, 1989; Ferrer and Perera 1988; Deacon 1990).

The two atypical spiny neurons types traced in the giraffe, horizontal pyramidal and crab-like neurons, both appear to facilitate horizontal integration within the cortex based on the domain covered by their dendritic arrays (van Brederode et al. 2000). Consistent with reports in carnivores, artiodactyls, and primates, horizontal pyramidal neurons in the giraffe were located mainly in deep regions of the sulcus (Ferrer et al.1986b). Horizontal pyramidal neurons have been documented in several species at various cortical depths (bat, rat, dog: Ferrer et al. 1986b; Ferrer 1987; human: Meyer 1987; rodents: Miller 1988; elephant: Jacobs et al. 2011), including a variety of cetaceans (Kraus and Pilleri 1969a, b; Garey et al. 1985; Ferrer and Perera 1988). Giraffe horizontal neurons tended to be smaller (in terms of Vol and TDL) but similar in morphology to those observed in the deep cortical layers of minke and humpback whales (Butti et al. 2014b). In the giraffe, however, these neurons are located over a broader range of cortical depths (600–2,900 μm). As in minke and humpback whales, the giraffe horizontal pyramidal neurons express roughly the same dendritic extent as pyramidal neurons, with a basilar array that appears more extensive than that observed in layer VI of several other species (Ferrer et al. 1986a, b). The axons of the giraffe horizontal neurons travel parallel with the apical dendrite, much as depicted in the dog and sheep (Figs. 6 and 9 in Ferrer et al. 1986a), further indicating horizontal integration within the cortex. In contrast to the horizontal pyramidal neuron, the crab-like neuron appears to have no counterpart in the cetacean

neocortex (Butti et al. 2014b), although such a limited sample from a Golgi impregnation is far from conclusive. At this point, we cannot rule out that these neurons may be (a variant of) spiny stellate neurons (White and Rock 1980; Lübke et al. 2000), and their location in the middle of the visual cortex is consistent with this possibility. Similar, albeit larger versions of these neurons have been documented in the elephant cerebral cortex (Jacobs et al. 2011). Although precise function of these crab-like neurons remains unknown, they resemble the bipolar neurons (Fig. 9 in Ferrer et al. 1986b) and atypical pyramidal neurons with multiple horizontal branches (Fig. 6 in Ferrer et al. 1986b) described in the sheep and dog.

The qualitative characteristics of these spiny neurons in the giraffe lead to two general observations. First, apical dendritic morphology in the giraffe cortex closely resembles that in cetaceans (Butti et al. 2014b) insofar as most apical dendrites are either singular, or narrowly bifurcating after considerable distance from the soma. This is markedly different from the widely bifurcating, V-shaped apical dendrites documented in the elephant (Jacobs et al. 2011, Fig. 10). As such, at least some cetartiodactyls appear to fall between the largely single apical dendritic architecture exhibited by anthropoid primate and murid rodents (Escobar et al. 1986; Meyer 1987; de Lima et al. 1990; Innocenti and Vercelli 2010) and the widely bifurcating apical dendritic structure exhibited by elephants (Jacobs et al. 2011). Second, despite many similarities in spiny neurons between giraffes and cetaceans, there are also some clear differences insofar as several spiny neuron types documented in cetaceans do not appear in the present sample: (1) atypical variations of a variety of documented pyramidal neurons (i.e., inverted, flattened, multiapical, bitufted, and tri-tufted; Ferrer and Perera 1988; Marino et al. 2007; Butti et al. 2014b), and (2) Sternzelle, a multipolar, apical-less neuron that appears to be specific to the cetacean neocortex (Kraus and Pilleri 1969b). Such neuromorphological differences within cetartiodactyls, if real rather than the result of sampling biases, should not be surprising as clear differences in the complement of neuron morphological types have also been documented in the neocortex within other clades (e.g., Afrotheria, Bianchi et al. 2011).

Aspiny neurons

The current findings are consistent with the observation that the dendritic morphology of aspiny neurons appears highly conserved among mammals (Hof et al. 1999; Sherwood et al. 2009). Giraffe aspiny interneurons in the present sample were characterized by several well-recognized dendritic morphologies (e.g., multipolar, bitufted, and neurogliaform), which have been identified in several species (Ferrer et al. 1986a, b; Hassiotis and Ashwell 2003; Povysheva et al. 2007; Bianchi et al. 2011; Jacobs et al. 2011), including cetaceans (Garey et al. 1985; Ferrer and Perera 1988; Butti et al. 2014b). These morphologies were similar across both primary motor and visual cortices. Quantitatively, the Vol and TDL of aspiny neurons in the giraffe were generally much smaller than in the humpback whale (Butti et al. 2014b). Giraffe multipolar and bitufted aspiny neurons had extensive dendritic radii (~500–600 μm, Fig. 8g) that are generally longer than documented in the rat (50–400 μm, Kawaguchi 1995), cat (50–400 μm, Peters and Regidor 1981; Somogyi et al. 1983), and echidna (100–400 μm, Hassiotis and Ashwell 2003). In comparison to cetaceans, the giraffe aspiny dendritic radius was longer than documented in the striped dolphin (100–300 μm, Ferrer and Perea 1988), bottlenose dolphin (~300 μm), and minke whale (~300–375 μm; Butti et al. 2014b), and about the same as that observed in the humpback whale (~470–575 μm, Butti et al. 2014b). The giraffe aspiny dendritic radius is roughly comparable to that observed in humans (~500–8,000 μm, Meyer 1987; Kisvárday et al. 1990) and macaque monkeys (~500 μm, Lund and Lewis 1993), but smaller than the 1,000-μm length in the elephant (Jacobs et al. 2011).

Similar results obtained for the giraffe neurogliaform neurons, which appear to be larger than reported in some species (e.g., cat: Thompson and Bannister 2003; rat and monkey: Povysheva et al. 2007) but smaller than those observed in the elephant (Jacobs et al. 2011). In the present sample and consistent with the observations of Ferrer et al. (1986b), they exhibited many more primary dendritic branches than did other aspiny neurons, but their dendrites tended to be shorter. Comparison with cetacean neurogliaform neurons is not possible because there is only minimal reference to the possibility of this neuronal type in cetaceans (Glezer and Morgane 1990). Finally, the relatively large size of these giraffe interneurons, which are presumably γ-aminobutyric acid-(GABA-) ergic (Kisvárday et al. 1986; Hof et al. 1996; The Petilla Interneuron Nomenclature Group et al. 2008), suggests the possibility of widespread inhibitory influences during cortical processing (Constantinidis et al. 2002).

Regional variation between giraffe motor and visual cortices

Although spiny neurons in motor cortex tended to exhibit greater dendritic extent and spine numbers than in visual cortex, there were too few of each neuronal type to allow for meaningful statistical comparisons. Even for pyramidal neurons, the differences in distribution measures among the four clusters demonstrated considerable variability in giraffe neuronal morphology. This conclusion

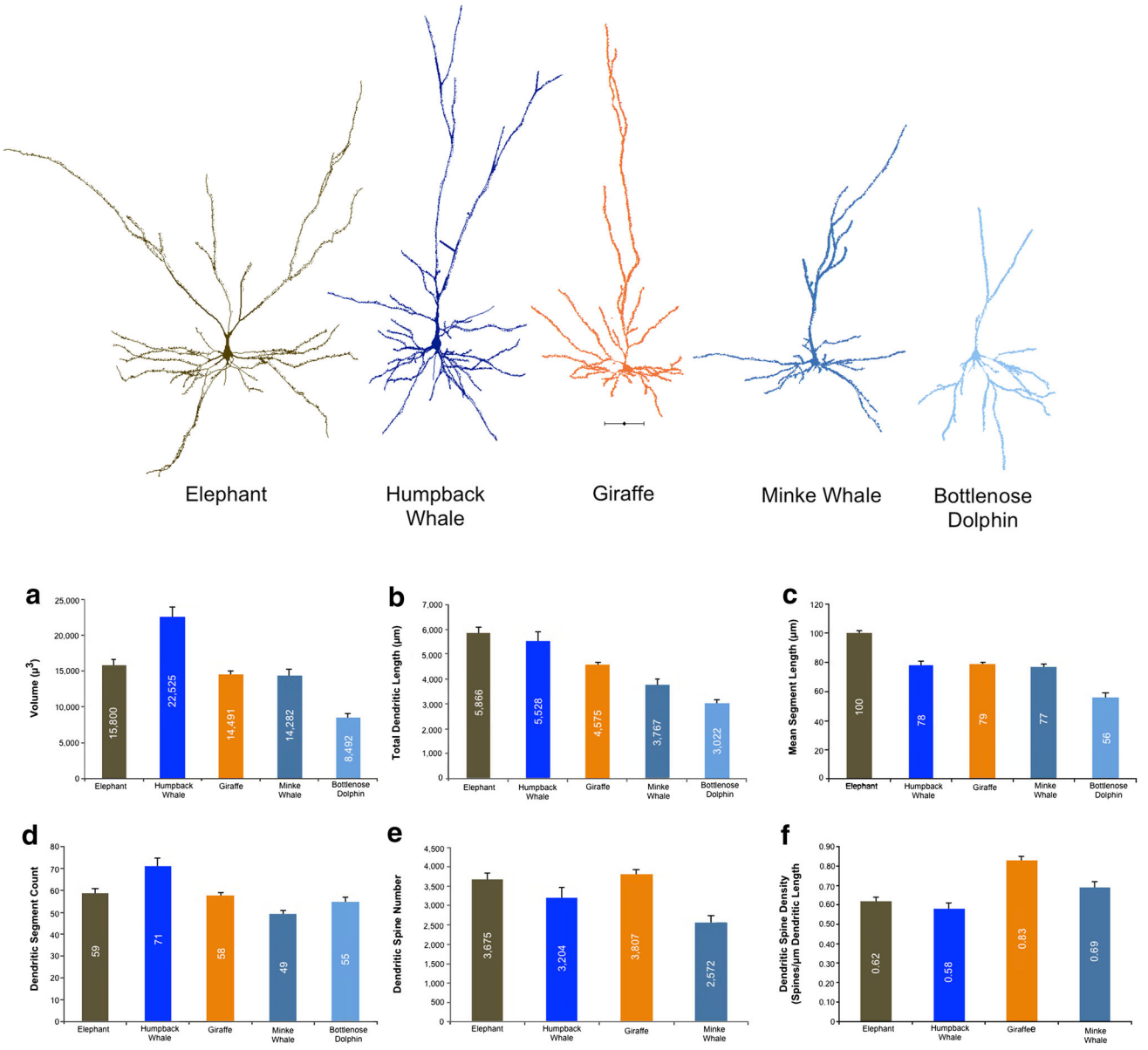

Fig. 10 Neurolucida tracings of representative pyramidal neurons in the frontal cortex of the elephant, visual cortex in humpback whale, giraffe, and minke whale, and in anterior temporal cortex of bottlenose dolphin. Note the widely bifurcating apical dendrite in the elephant and the more narrowly bifurcating apical dendrites in cetartioldactyls. Neurons were chosen to represent the approximate averages for each species in terms of total dendritic length. Dependent measures of typical pyramidal neurons across each species are presented in *bar graphs* for relative Vol (**a**), total dendritic length, TDL (**b**), mean segment length, MSL (**c**), dendritic segment count, DSC (**d**), dendritic spine number, DSN (**e**), and dendritic spine density, DSD (**f**). Note that the elephant data represent only superficial pyramidal neurons. Quantitative dendritic measures (Vol, TDL, MSL, DSC) indicate that the elephant and humpback whale generally had more extensive dendrites than giraffes, whereas minke whale and bottlenose dolphin had less extensive dendritic arbors. Spine measures (DSN, DSD) were highest in the giraffe and elephant, perhaps due to perfusion fixation and stain quality. Note that DSN and DSD for the bottlenose dolphin are not included due to poor impregnation. *Scale bar* 100 μm

was futher supported by the significant differences in the decision tree results. The inability to fit models to the current giraffe data thus suggests that there are multiple sources of dendritic measure variability, and that the present results may be due to actual neural differences and/or may be artifacts of staining.

Quantitative comparison of pyramidal neurons across species

To further our understanding of the quantitative morphological characteristics of giraffe cortical neurons, we compared the current results with those from other species

Table 4 Demographics of species in pyramidal neuron comparisons arranged by brain mass (high to low)

	Elephant[a]	Humpback Whale[b]	Minke Whale[b]	Bottlenose Dolphin[b]	Giraffe
Age/sex	20–30 year-old adult males ($n = 2$)	Juvenile male ($n = 1$)	Young female ($n = 1$)	Adult, unknown age/gender ($n = 1$)	Sub-adult male ($n = 3$)
Fixation method[c]	Perfusion	Immersion (AT < 8 h)	Immersion (AT < 48 h)	Immersion (AT < 2 h)	Perfusion
Region sampled[d]	RH visual and frontal cortices	LH visual, frontal, anterior, and posterior temporal cortices	LH visual and motor cortices	LH visual and anterior temporal cortices	RH motor and visual cortices
$Mean_{Soma\ depth}$ (μm)[e]	794 ± 289	1,173 ± 327	1,222 ± 575	792 ± 289	988 ± 419
$Mean_{Brain\ mass}$ (g)	4,990	3,603	1,810	1,250	539
$Mean_{Soma\ size}$ (μm^2)[f]	516 ± 123	524 ± 98	370 ± 84	357 ± 140	324 ± 96
$n_{Pyramidal\ neurons}$	40	20	24	33	143

[a] From Jacobs et al. (2011)

[b] From Butti et al. (2014b)

[c] *AT* autolysis time

[d] *RH* right hemisphere, *LH* left hemisphere

[e] The soma depth (mean ± SD) in the elephant is less because only superficial (as opposed to deeper) pyramidal neurons were included

[f] Soma size is represented by mean ± SD

quantified with the same methodology. Specifically, we compared the dendritic morphology of pyramidal neurons in the giraffe with the same measurements obtained from pyramidal neurons in different cortical regions of the African elephant and three cetacean species (bottlenose dolphin, minke whale, and humpback whale; see Table 4). Although these are clearly not ideal comparisons due to the number of uncontrolled factors (e.g., small sample size, subjects of different ages, regional and associated functional cortical variations, perfusion vs. immersion fixation), methodologically similar quantitative analyses provide at least a preliminary, relative measure for such comparisons among these species.

A total of 260 pyramidal neurons were compared for dendritic (Vol, TDL, MSL, DSC) and spine (DSN, DSD) measures, as well as for soma size (Table 4). Results are summarized graphically in Fig. 10. In terms of Vol, the humpback whale had much higher values than the other species, with the dolphin being the lowest (Fig. 10a). TDL revealed the giraffe to be roughly in the middle, the elephant and humpback whale at the upper end, and the minke whale and bottlenose dolphin at the lower end (Fig. 10b). MSL was lowest in the dolphin, but was much higher in the elephant than in the other species (Fig. 10c), which is consistent with previous observations suggesting that cortical neurons in the elephant are characterized by less branchy but particularly long dendrites (Jacobs et al. 2011). For DSC, the humpback whale value was higher than all of the other species, with the minke whale being lowest (Fig. 10d). Elephant and especially giraffe pyramidal neurons generally exhibited the highest spine values (Fig. 10e, f), perhaps reflecting the quality of the perfusion fixation used for these brains, and subsequent high stain quality, over the immersion fixation for the cetacean brains (Morest and Morest 2005).

Although dendritic systems may scale with brain size within a particular lineage (Elston et al. 2006; Elston and Manger 2014), and although we have previously documented a consistent positive correlation between soma size and dendritic extent in humans (Jacobs et al. 2001, 2011), individual dendritic and spine measures do not consistently differentiate the species in the present sample. The current data cannot resolve whether dendritic measures scale with brain size across these diverse species, in part because (1) a confluence of several dendritic/spine measures may be needed to detect species differences (Jacobs et al. 2014), and/or (2) dendritic and especially spine measures are confounded by differential fixation and stain quality across brains. Nevertheless, there does appear to be a positive relationship between brain mass and soma size in some studies (Haug 1987; Purves 1988; Changizi 2001; Sherwood et al. 2003). In the present sample, soma size and brain mass increased in a similar manner (Table 4): giraffe < dolphin < minke whale < elephant and humpback whale. Indeed, a Spearman's rho correlation between soma size and brain mass was positive ($r_{(260)} = 0.52$, $p = 0.0001$). Further, Spearman's rho correlations between soma size and dendritic measures were positive for all measures except DSD (Vol: $r_{(260)} = 0.62$, $p = 0.0001$; TDL: $r_{(260)} = 0.49$, $p = 0.0001$; MSL: $r_{(260)} = 0.34$, $p = 0.0001$; DSC: $r_{(260)} = 0.32$, $p = 0.0001$; DSN: $r_{(260)} = 0.20$, $p = 0.001$; DSD: $r_{(260)} = -0.19$, $p = 0.002$). These findings contribute to existing data on the relationship between neuronal measures and brain

mass, a multifaceted relationship complicated by functional design principles and lineage-specific deviations (Haug 1987; Kaas 2000; Changizi 2001; Elston et al. 2001; Harrison et al. 2002; Wittenberg and Wang 2007).

In conclusion, the present study provides the first documentation of neuronal morphology in the giraffe neocortex, which exhibits a variety of extensively spiny neuron types arranged in a predominantly vertically oriented cortical architecture. Several similarities appear to exist between the giraffe and other cetartiodactyls. In particular, giraffe cortices, like those in cetaceans, but not other artiodactyls, exhibit pyramidal neurons with either singular or narrowly bifurcating apical dendritic shafts, and superficial layers that contain extraverted neurons. However, clear differences between giraffe and cetacean cortices are also apparent in the relative presence/absence of Sternzelle, neurogliaform neurons, crab-like neurons, and several pyramidal neuron variants (e.g. the tri-tufted pyramidal neuron). In these ways, giraffes may be more closely aligned with other artiodactyls than they are to cetaceans, although more comparative research is clearly required. Quantitatively, pyramidal neuron morphometry tentatively places giraffes in the middle of a cross-species comparison for dendritic measures, with the elephant and the humpback whale at the upper end, and the minke whale and dolphin at the lower end. Nevertheless, data are limited at this point because of methodological issues, with more extensive neuromorphological studies across a variety of large brained mammals of different brain sizes required for a clearer picture to emerge.

Acknowledgments Partial support for this work was provided by Colorado College's divisional research funds (B.J.), the James S. McDonnell Foundation (Grant 22002078, to C.C.S., P.R.H.; Grant 220020293 to C.C.S.), National Science Foundation (BCS-0515484, BCS-0824531 to C.C.S.), and the South African National Research Foundation (P.R.M.; FA2005033100004). We would also like to thank the Danish Cardiovascular Research Program, especially Emil Toft-Brøndum, for allowing us to obtain the specimens of giraffe brains.

References

Anderson K, Bones B, Robinson B, Hass C, Lee H, Ford K, Roberts T-A, Jacobs B (2009) The morphology of supragranular pyramidal neurons in the human insular cortex: a quantitative Golgi study. Cereb Cortex 19:2131–2144

Badeer HS (1997) Is the flow in the giraffe's jugular vein a "free" fall? Comp Biochem Physiol A 118:573–576

Badlangana NL, Bhagwandin A, Fuxe K, Manger PR (2007a) Distribution and morphology of putative catecholaminergic and serotonergic neurons in the medulla oblongata of a sub adult giraffe, *Giraffa camelopardalis*. J Chem Neuroanat 34:69–79

Badlangana NL, Bhagwandin A, Fuxe K, Manger PR (2007b) Observations on the giraffe central nervous system related to the corticospinal tract, motor cortex and spinal cord: what difference does a long neck make? Neurosci 148:522–534

Badlangana NL, Adams JW, Manger PR (2009) The giraffe (*Giraffa camelopardalis*) cervical vertebral column: a heuristic example in understanding evolutionary processes? Zool J Linn Soc 155:736–757

Barasa A (1960) Forma, grandezza e densitá dei neuroni della corteccia cerebrale in mammiferi di grandezza corporea differente. Z Zellforsch 53:69–89

Bashaw MJ (1993) Social behavior and communication in a heard of captive giraffe. Dissertation, Georgia Institute of Technology

Bashaw MJ, Bloomsmith MA, Maple TL, Bercovitch FB (2007) The structure of social relationships among captive female giraffe (*Giraffe camelopardalis)*. J Comp Psychol 121:46–53

Bercovitch FB, Berry PSM (2013) Herd composition, kinship and fission-fusion social dynamics among wild giraffe. Afr J Ecol 51:206–216

Bercovitch FB, Bashaw MJ, del Castillo SM (2006) Sociosexual behavior, male mating tactics, and the reproductive cycle of giraffe *Giraffa camelopardalis*. Horm Behav 50:314–321

Betz W (1874) Anatomischer Nachweis zweier Gehirncentra. Zbl med Wiss 12(578–580):595–599

Bianchi S, Bauernfeind AL, Gupta K, Stimpson CD, Spocter MA, Bonar CJ, Manger PR, Hof PR, Jacobs B, Sherwood CC (2011) Neocortical neuron morphology in Afrotheria: comparing the rock hyrax with the African elephant. Ann NY Acad Sci 1225:37–46

Boddy AM, McGowen MR, Sherwood CC, Grossman LI, Goodman M, Wildman DE (2012) Comparative analysis of encephalization in mammals reveals relaxed constraints on anthropoid primate and cetacean brain scaling. J Evol Biol 25:981–994

Bok ST (1959) Histonomy of the cerebral cortex. Elsevier, Amsterdam

Bota M, Swanson LW (2007) The neuron classification problem. Brain Res Rev 56:79–88

Braak H (1978) On magnopyramidal temporal fields in the human brain—probable morphological counterparts of Wernicke's speech region. Anat Embryol 152:141–169

Braak H, Braak E (1976) The pyramidal cells of Betz within the cingulate and precentral gigantopyramidal field in the human brain: a Golgi and pigmentarchitectonic study. Cell Tiss Res 172:103–119

Braak H, Braak E (1985) Golgi preparations as a tool in neuropathology with particular reference to investigations of the human telencephalic cortex. Prog Neurobiol 25:93–139

Brodmann K (1909) Vergleichende Lokalisationlehre der Grosshirnrinde in ihren Prinzipien dargestellt auf Grund des Zellenbaues. J. A. Barth, Leipzig

Butti C, Raghanti MA, Sherwood CC, Hof PR (2011) The neocortex of cetaceans: cytoarchitecture and comparison with other aquatic and terrestrial species. Ann NY Acad Sci 1225:47–58

Butti C, Fordyce ER, Raghanti MA, Gu X, Bonar CJ, Wicinski BA, Wong EW, Roman J, Brake A, Eaves E, Spocter MA, Tang CY, Jacobs B, Sherwood CC, Hof PR (2014a) The cerebral cortex of the pygmy hippopotamus, *Hexaprotodon liberiensis* (Cetartiodactyla, Hippopotamidae): MRI, cytoarchitecture, and neuronal morphology. Anat Rec 297:670–700

Butti C, Janeway CM, Townshend C, Ridgway SH, Manger PR, Sherwood CC, Hof PR, Jacobs B (2014b) Neuronal morphology in cetartiodactyls. I. A comparative Golgi analysis of neuronal morphology in the bottlenose dolphin (*Tursiops truncatus*), the minke whale (*Balaenoptera acutorostrata*), and the humpback whale (*Megaptera novaeangliae*). Brain Struct Funct (submitted)

Bux F, Bhagwandin A, Fuxe K, Manger PR (2010) Organization of cholinergic, putative catecholaminergic and serotonergic nuclei

in the diencephalon, midbrain and pons of sub-adult male giraffes. J Chem Neuroanat 39:189–203
Carter KD, Seddon JM, Frère CH, Carter JK, Goldizen AW (2012) Fission-fusion dynamics in wild giraffes may be driven by kinship, spatial overlap and individual social preferences. Anim Behav 85:385–394
Changizi MA (2001) Principles underlying mammalian neocortical scaling. Biol Cybern 84:207–215
Chan-Palay V, Palay SL, Billings-Gagliardi SM (1974) Meynert cells in primate visual cortex. J Neurocytol 3:631–658
Clemo HR, Meredith MA (2012) Dendritic spine density in multisensory versus primary sensory cortex. Synapse 66:714–724
Coe MJ (1967) "Necking" behavior in the giraffe. J Zool Lond 151:313–321
Coimbra JP, Hart NS, Collin SP, Manger PR (2013) Scene from above: retinal ganglion cell topography and spatial resolving power in the giraffe (*Giraffa camelopardalis*). J Comp Neurol 521:2042–2057
Constantinidis C, Williams GC, Goldman-Rakic PS (2002) A role for inhibition in shaping the temporal flow of information in prefrontal cortex. Nat Neurosci 5:175–180
Cozzi B, Povinelli M, Ballarin C, Granato A (2014) The brain of the horse: weight and cephalization quotients. Brain Behav Evol 83:9–16
Crawford JM, Curtis DR (1966) Pharmacological studies on feline Betz cells. J Physiol 186:121–138
Crile G, Quiring DP (1940) A record of the body weight and certain organ and gland weights of 3690 animals. Ohio J Sci 40:219–259
de Lima AD, Voigt T, Morrison JH (1990) Morphology of the cells within the inferior temporal gyrus that project to the prefrontal cortex in the macaque monkey. J Comp Neurol 296:159–172
Deacon TW (1990) Rethinking mammalian brain evolution. Am Zool 30:629–705
DeFelipe J, Alonso-Nanclares L, Arellano JI (2002) Microstructure of the neocortex: comparative aspects. J Neurocytol 31:299–316
DeFelipe J, López-Cruz PL, Benavides-Piccione R, Bielza C, Larrañaga P, Anderson S, Burkhalter A, Cauli B, Fairén A, Feldmeyer D, Fishell G, Fitzpatrick D, Freund TF, González-Burgos G, Hestrin S, Hill S, Hof PR, Huang J, Jones EG, Kawaguchi Y, Kisvárday Z, Kubota Y, Lewis DA, Marín O, Markram H, McBain CJ, Meyer HS, Monyer H, Nelson SB, Rockland K, Rossier J, Rubenstein JLR, Rudy B, Scanziani M, Shepherd GM, Sherwood CC, Staiger JF, Tamás G, Thomson A, Wang Y, Yuste R, Ascoli GA (2013) New insights into the classification and nomenclature of cortical GABAergic interneurons. Nat Rev Neurosci 14:202–216
Dell L-H, Patzke N, Bhagwandin A, Bux F, Fuxe K, Barber G, Siegel JM, Manger PR (2012) Organization and number of orexinergic neurons in the hypothalamus of two species of Cetartiodactyla: a comparison of giraffe (*Giraffa camelopardalis*) and harbour porpoise (*Phocoena phocoena*). J Chem Neuroanat 44:98–109
Elston GN (2003) Cortex, cognition and the cell: new insights into the pyramidal neuron and prefrontal function. Cereb Cortex 13:1124–1138
Elston GN (2007) Specialization of the neocortical pyramidal cell during primate evolution. In: Kass JH, Preuss TM (eds) Evolution of nervous systems: a comprehensive reference, vol 4. Elsevier, New York, pp 191–242
Elston GN, Manger P (2014) Pyramidal cells in V1 of African rodents are bigger, more branched and more spiny than those in primates. Front Neuroanat 8:4. doi:10.3389/fnana.2014.00004
Elston GN, Rosa MGP (1998a) Complex dendritic fields of pyramidal cells in the frontal eye field of the macaque monkey: comparison with parietal areas 7a and LIP. Neuroreport 9:127–131
Elston GN, Rosa MGP (1998b) Morphological variation of layer III pyramidal neurones in the occipitotemporal pathway of the macaque monkey visual cortex. Cereb Cortex 8:278–294
Elston GN, Benavides-Piccione R, DeFelipe J (2001) The pyramidal cell in cognition: a comparative study in human and monkey. J Neurosci 21:RC163
Elston GN, Benavides-Piccione R, Elston A, Zietsch B, Defelipe J, Manger P, Casagrande V, Kaas JH (2006) Specializations of the granular prefrontal cortex of primates: implications for cognitive processing. Anat Rec 288:26–35
Escobar MI, Pimienta H, Caviness VS Jr, Jacobson M, Crandall JE, Kosik KS (1986) Architecture of apical dendrites in the murine neocortex: dual apical dendritic systems. Neuroscience 17:975–989
Fernández MA, Vrba ES (2005) A complete estimate of the phylogenetic relationships in Ruminantia: a dated species-level supertree of the extant ruminants. Biol Rev 80:269–302
Ferrer I (1987) The basic structure of the neocortex in insectivorous bats (*Miniopterus sthreibersi* and *Pipistrellus pipistrellus*). J Hirnforsch 28:237–243
Ferrer I (1989) The basic structure of the neocortex of the bat. Neurosci Res 6:573–580
Ferrer I, Perera M (1988) Structure and nerve organization in the cerebral cortex of the dolphin *Stenella coeruleoalba* a Golgi study: with special attention to the primary auditory area. Anat Embryol 178:161–173
Ferrer I, Fábrigues I, Condom E (1986a) A Golgi study of the sixth layer of the cerebral cortex I. The lissencephalic brain of Rodentia, Lagomorpha. Insectivora and Chiroptera. J Anat 145:217–234
Ferrer I, Fábrigues I, Condom E (1986b) A Golgi study of the sixth layer of the cerebral cortex II. The gyrencephalic brain of Carnivora. Artiodactyla and primates. J Anat 146:87–104
Friant M (1968) Développement et morphologie du cerveau des giraffidae (Okapi et Girafe) [The development and morphology of the brain of giraffidae (okapi and giraffe)]. Acta Neurol Belg 68:483–498
Garey LJ, Winkllemann E, Brauer K (1985) Golgi and Nissl studies of the visual cortex of the bottlenose dolphin. J Comp Neurol 240:305–321
Germroth P, Schwerdtfeger WK, Buhl EH (1989) Morphology of identified entorhinal neurons projecting to the hippocampus. A light microscopical study combining retrograde tracing and intracellular injection. Neuroscience 30:683–691
Glezer II, Morgane PJ (1990) Ultrastructure of synapses and Golgi analysis of neurons in neocortex of the lateral gyrus (visual cortex) of the dolphin and pilot hale. Brain Res Bull 24:401–427
Graur D, Higgins DG (1994) Molecular evidence for the inclusion of cetaceans within the order Artiodactyla. Mol Biol Evol 11:357–364
Harrison KH, Hof PR, Wang SS-H (2002) Scaling laws in the mammalian neocortex: does form provide clues to function? J Neurocytol 31:289–298
Hassanin A, Douzery EJP (2003) Molecular and morphological phylogenies of Ruminantia and the alternative position of the Moschidae. Syst Biol 52:206–228
Hassiotis M, Ashwell KWS (2003) Neuronal classes in the isocortex of a monotreme, the Australian echidna (*Tachyglossus aculeatus*). Brain Behav Evol 61:6–27
Haug H (1987) Brain sizes, surfaces, and neuronal sizes of the cortex cerebri: a stereological investigation of man and his variability and a comparison with some mammals (primates, whales, marsupials, insectivores, and one elephant). Am J Anat 180:126–142

Hawkins DM, Kass GV (1982) Automatic interaction detection. In: Hawkins D (ed) Topics in applied multivariate analysis. University of Cambridge Press, Cambridge, pp 269–302

Hayes TL, Lewis DA (1995) Anatomical specialization of the anterior motor speech area: hemispheric differences in magnopyramidal neurons. Brain Lang 49:289–308

Hof PR, Sherwood CC (2005) Morphomolecular neuronal phenotypes in the neocortex reflect phylogenetic relationships among certain mammalian orders. Anat Rec 287:1153–1163

Hof PR, Sherwood CC (2007) The evolution of neuron classes in the neocortex of mammals. In: Krubitzer LA, Kaas H (eds) The evolution of nervous systems in mammals. Evolution of nervous systems, vol 3. Academic Press, Oxford pp 113–124

Hof PR, Van der Gucht E (2007) Structure of the cerebral cortex of the humpback whale, *Megaptera novaeangliae* (Cetacea, Mysticeti, Balaenopteridae). Anat Rec 290:1–31

Hof PR, Bogaert YE, Rosenthal RE, Fiskum G (1996) Distribution of neuronal populations containing neurofilament protein and calcium-binding proteins in the canine neocortex: regional analysis and cell typology. J Chem Neuroanat 11:81–98

Hof PR, Glezer II, Condé F, Flagg RA, Rubin MB, Nimchinsky EA, Vogt Weisenhorn DM (1999) Cellular distribution of the calcium-binding proteins parvalbumin, calbindin, and calretinin in the neocortex of mammals: phylogenetic and developmental patterns. J Chem Neuroanat 16:77–116

Hof PR, Nimchinsky EA, Young WG, Morrison JH (2000) Numbers of meynert and layer IVB cells in area V1: a stereologic analysis in young and aged macaque monkeys. J Comp Neurol 420:113–126

Hof PR, Chanis R, Marino L (2005) Cortical complexity in cetacean brains. Anat Rec 287A:1142–1152

Horner CH, Arbuthnott E (1991) Methods of estimation of spine density—are spines evenly distributed throughout the dendritic field? J Anat 177:179–184

Innis AC (1958) The behavior of the giraffe, *Giraffa camelopardalis*, in the eastern Transvaal. Proc Zool Soc Lond 131:245–278

Innocenti GM, Vercelli A (2010) Dendritic bundles, minicolumns, columns, and cortical output units. Front Neuroanat 4:11. doi:10.3389/neuro.05.011.2010

Jacobs B, Scheibel AB (1993) A quantitative dendritic analysis of Wernicke's area in humans I. Lifespan changes. J Comp Neurol 327:83–96

Jacobs B, Scheibel AB (2002) Regional dendritic variation in primate cortical pyramidal cells. In: Schuz A, Miller R (eds) Cortical areas: unity and diversity (conceptual advances in brain research series). Taylor & Francis, London, pp 111–131

Jacobs B, Schall M, Scheibel AB (1993) A quantitative dendritic analysis of Wernicke's area in humans II. Gender, hemispheric, and environmental factors. J Comp Neurol 327:97–111

Jacobs B, Driscoll L, Schall M (1997) Life-span dendritic and spine changes in areas 10 and 18 of human cortex: a quantitative Golgi study. J Comp Neurol 386:661–680

Jacobs B, Schall M, Prather M, Kapler E, Driscoll L, Baca S (2001) Regional dendritic and spine variation in human cerebral cortex: a quantitative Golgi study. Cereb Cortex 11:558–571

Jacobs B, Lubs J, Hannan M, Anderson K, Butti C, Sherwood CC, Hof PR, Manger PR (2011) Neuronal morphology in the African elephant (*Loxodonta africana*) neocortex. Brain Struct Funct 215:273–298

Jacobs B, Johnson N, Wahl D, Schall M, Maseko BC, Lewandowski A, Raghanti MA, Wicinski B, Butti C, Hipkins WD, Bertelsen MF, Reep RL, Hof PR, Sherwood CC, Manger PR (2014) Comparative neuronal morphology of cerebellar cortex in afrotherians (African elephant, Florida manatee), primates (human, common chimpanzee), cetartiodactyls (humpback whale, giraffe), and carnivores (Siberian tiger, clouded leopard). Front Neuroanat 8:24. doi:10.3389/fnana.2011.00024

Kaas JH (2000) Why is brain size so important: design problems and solutions as neocortex gets bigger or smaller. Brain Mind 1:7–23

Kaiserman-Abramof IR, Peters A (1972) Some aspects of the morphology of Betz cells in the cerebral cortex of the cat. Brain Res 43:527–546

Kawaguchi Y (1995) Physiological subgroups of nonpyramidal cells with specific morphological characteristics in layer II/III of rat frontal cortex. J Neurosci 15:2638–2665

Kisvárday ZF, Cowey A, Somogyi P (1986) Synaptic relationships of a type of GABA-immunoreactive neuron (clutch cell), spiny stellate cells and lateral geniculate nucleus afferents in layers IVC of the monkey striate cortex. Neurosci 19:741–761

Kisvárday ZF, Gulyas A, Beroukas D, North JB, Chub IW, Somogyi P (1990) Synapses, axonal and dendritic patterns of GABA-immunoreactive neurons in human cerebral cortex. Brain 113:793–812

Kraus C, Pilleri G (1969a) Zur Feinstruktur der groβen Pyramidenzellen in der V. Cortexschicht der Cetacean (*Delphinus delphins* und *Balaenoptera borealis)*. Z Mikrosk Anat Forsch 80:89–99

Kraus C, Pilleri G (1969b) Zur Histologie der Grosshirnrinde von *Balaenoptera borealis* (*Cetacea, Mysticeti*) Invest Cetacea 1:151–170

le Gros Clark WE (1942) The cells of Meynert in the visual cortex of the monkey. J Anat 76:369–376

Lu D, He L, Xiang W, Ai W-M, Cao Y, Wang X-S, Pan A, Luo X-G, Li Z, Yan X–X (2013) Somal and dendritic development of human CA3 pyramidal neurons from midgestation to middle childhood: a quantitative Golgi study. Anat Rec 296:123–132

Lübke J, Egger V, Sakmann B, Feldmeyer D (2000) Columnar organization of dendrites and axons of single and synaptically coupled excitatory spiny neurons in layer 4 of the rat barrel cortex. J Neurosci 10:5300–5311

Lund JS, Lewis DA (1993) Local circuit neurons of the developing mature macaque prefrontal cortex: Golgi and immunocytochemical characteristics. J Comp Neurol 328:282–312

Manger PR, Cort J, Ebrahim N, Goodman A, Henning J, Karolia M, Rodrigues S-L, Strkalj G (2008) Is 21st century neuroscience too focused on the rat/mouse model of the brain function and dysfunction? Front Neuroanat 2:5. doi:10.3389/neuro.05.005.2008

Manger PR, Pillay P, Maseko BC, Bhagwandin A, Gravett N, Moon D-J, Jillani N, Hemingway J (2009) Acquisition of brains from the African elephant (*Loxodonta africana*): perfusion-fixation and dissection. J Neurosci Methods 179:16–21

Marino L, Connor RC, Fordyce RE, Herman LM, Hof PR, Lefebvre L, Lusseau D, McCowan B, Nimchinsky EA, Pack AA, Rendell L, Reidenberg JS, Reiss D, Uhen MD, Van der Gucht E, Whitehead H (2007) Cetaceans have complex brains for complex cognition. PLoS Biol 5:966–972

Masland RH (2004) Neuronal cell types. Curr Biol 14:R497–R500

Meyer G (1987) Forms and spatial arrangement of neurons in the primary motor cortex of man. J Comp Neurol 262:402–428

Meynert T (1867) Der Bau der Gross-Hirnrinde und seiner örtlichen Verschiedenheiten, nebst einen pathologisch-anatomisch Corollarium. Vierteljahrsschr Psychiatr 1(77–93):125–217

Miller MW (1988) Maturation of rat visual cortex: IV. The generation, migration, morphogenesis and connectivity of atypical oriented pyramidal cells. J Comp Neurol 274:387–405

Mitchell G, Bobbitt JP, Devries S (2008) Cerebral perfusion pressure in giraffe: modeling the effects of head-raising and -lowering. J Theor Biol 252:98–108

Morest DK, Morest RR (2005) Perfusion-fixation of the brain with chrome-osmium solutions for the rapid Golgi method. Am J Anat 118:811–831

Morgane PJ, Jacobs MS, Galaburda A (1985) Conservative features of neocortical evolution in dolphin brain. Brain Behav Evol 26:176–184

Morgane PJ, Glezer LI, Jacobs MS (1988) Visual cortex of the dolphin: an image analysis study. J Comp Neurol 273:3–25

Mountcastle VB (1997) The columnar organization of the neocortex. Brain 120:701–722

Murphy WJ, Pevzner PA, O'Brien SJ (2004) Mammalian phylogenomics comes of age. Trends Genet 20:631–639

Nelson SB, Sugino K, Hempel CM (2006) The problem of neuronal cell types: a physiological genomics approach. Trends Neurosci 29:339–345

Ngowyang G (1932) Beschreibung einer Art von Specialzellen in der Inselrinde. J Psychol Neurol 44:671–674

Nikaido M, Rooney AP, Okada N (1999) Phylogenetic relationships among cetartiodactyls based on insertions of short and long interspersed elements: hippopotamuses are the closest extant relatives of whales. Proc Natl Acad Sci USA 96:10261–10266

Nilsson O, Böööj S, Dahlström A, Hargens AR, Millard RW, Pettersson KS (1988) Sympathetic innervation of the cardiovascular system in the giraffe. Blood Vessels 25:299–307

Oelschläger HA (2008) The dolphin brain—a challenge for synthetic neurobiology. Brain Res Bull 75:450–459

Pérez-Barbería FJ, Gordon IJ (2005) Gregariousness increases brain size in ungulates. Oecologia 145:41–52

Peters A, Regidor J (1981) A reassessment of the forms of nonpyramidal neurons in area 17 of cat visual cortex. J Comp Neurol 203:685–716

Phillis JW, Limacher JJ (1974) Substance P excitation of cerebral cortical Betz cells. Brain Res 69:158–163

Povysheva NV, Zaitsev AV, Kröner S, Krimer OA, Rotaru DC, González-Burgos G, Lewis DA, Krimer LS (2007) Electrophysiological differences between neurogliaform cells from monkey and rat prefrontal cortex. J Neurophysiol 97:1030–1039

Price SA, Bininda-Edmonds ORP, Gittleman JL (2005) A complete phylogeny of whales, dolphins and even-toed hoofed mammals (cetartiodactyls). Biol Rev 80:445–473

Purves D (1988) Body and brain: a trophic theory of neural connections. Harvard University Press, Cambridge

Radinsky L (1981) Brain evolution in extinct South American ungulates. Brain Behav Evol 18:169–187

Ramón y Cajal S (1922) Studien über die Sehrinde der Katze. J Psychol Neurol 29:161–181

Rivara C, Sherwood C, Bouras C, Hof PR (2003) Stereological characterization and spatial distribution patterns of Betz cells in the human primary motor cortex. Anat Record 270:137–148

Roitman MF, Na E, Anderson G, Jones TA, Bernstein IL (2002) Induction of a salt appetite alters dendritic morphology in nucleus accumbens and sensitizes rats to amphetamine. J Neurosci 22:RC225 (1–5)

Sanides F, Sanides D (1972) The "extraverted neurons" of the mammalian cerebral cortex. Z Anat Entwickl-Gesch 136:272–293

Sasaki S, Iwata M (2001) Ultrastuctural study of Betz cells in the primary motor cortex of human brain. J Anat 199:699–708

Scheibel ME, Scheibel AB (1978a) The dendritic structure of the human Betz cell. In: Brazier MAB, Pets H (eds) Architectonics of the cerebral cortex. Raven Press, New York, pp 43–57

Scheibel ME, Scheibel AB (1978b) The methods of Golgi. In: Robertson RT (ed) Neuroanatomical research techniques. Academic Press, New York, pp 89–114

Sherwood CC, Lee PWH, Rivara CB, Holloway RL, Gilissen EPE, Simmons RMT, Hakeem A, Allman JM, Erwin JM, Hof PR (2003) Evolution of specialized pyramidal neurons in primate visual and motor cortex. Brain Behav Evol 61:28–44

Sherwood CC, Stimpson CD, Butti C, Bonar CJ, Newton AL, Allman JM, Hof PR (2009) Neocortical neuron types in Xenarthra and Afrotheria: implications for brain evolution in mammals. Brain Struct Funct 213:301–328

Shimamura M, Yasue H, Ohshima K, Abe H, Kato H, Kishiro T, Goto M, Munechika I, Okada N (1997) Molecular evidence from retroposons that whales form a clade within even-toed ungulates. Nature 388:666–671

Sholl DA (1953) Dendritic organization of the neurons of the visual and motor cortices of the cat. J Anat 87:387–406

Shultz S, Dunbar RIM (2006) Both social and ecological factors predict ungulate brain size. Proc R Soc B 273:207–215

Solounias N (1999) The remarkable anatomy of the giraffe's neck. J Zool (London) 247:257–268

Somogyi P, Kisvárday ZF, Martin KAC, Whitteridge D (1983) Synaptic connections of morphologically characterized large basket cells in the striate cortex of cat. Neuroscience 10:261–294

Tarou LR, Bashaw MJ, Maple TL (2000) Social attachment in giraffe: response to social separation. Zoo Biol 19:41–51

The Petilla Interneuron Nomenclature Group (PING) (2008) Petilla terminology: nomenclature of features of GABAergic interneurons of the cerebral cortex. Nat Rev Neurosci 9:557–568

Thompson AM, Bannister AP (2003) Interlaminar connections in the neocortex. Cereb Cortex 13:5–14

Tyler CJ, Dunlop SA, Lund RD, Harman AM, Dann JF, Beazley LD (1998) Anatomical comparison of the macaque and marsupial visual cortex: common features that may reflect retention of essential cortical elements. J Comp Neurol 400:449–468

Ursing BM, Arnason U (1998) Analyses of mitochondrial genomes strongly support a hippopotamus-whale clade. Proc R Soc Lond B265:2251–2255

Uylings HBM, Ruiz-Marcos A, van Pelt J (1986) The metric analysis of three-dimensional dendritic tree patterns: a methodological review. J Neurosci Methods 18:127–151

Valverde F (1971) Short axon neuronal subsystems in the visual cortex of the monkey. Int J Neurosci 1:181–197

van Brederode JFM, Foehring RC, Spain WJ (2000) Morphological and electrophysiological properties of atypically oriented layer 2 pyramidal cells of the juvenile rat neocortex. Neuroscience 101:851–861

Van der Jeugd HP, Prins HP (2000) Movements and group structure of giraffe (*Giraffa camelopardalis*) in Lake Manyara National Park, Tanzania. J Zool 251:15–21

von Bonin G (1938) Studies of the size of the cells in the cerebral cortex. II. The motor area of man, cebus and cat. J Comp Neurol 69:381–390

Walshe FM (1942) The giant cells of Betz, the motor cortex and the pyramidal tract: a critical review. Brain 65:409–461

White EL, Rock MP (1980) Three-dimensional aspects and synaptic relationships of a Golgi-impregnated spiny stellate cell reconstructed from serial thin sections. J Neurocytol 9:615–636

Williams RS, Ferrante RJ, Caviness VS Jr (1978) The Golgi rapid method in clinical neuropathology: the morphologic consequences of suboptimal fixation. J Neuropathol Exp Neurol 37:13–33

Wittenberg GM, Wang SS-H (2007) Evolution and scaling of dendrites. In: Stuart G, Spruston N, Hausser M (eds) Dendrites. Oxford University Press, New York, pp 43–67

Zeng H, Shen EH, Hohman JG, Oh SW, Bernard A, Royall JJ, Glattfelder KJ, Sunkin SM, Morris JA, Guillozet-Bongaarts AL, Smith KA, Ebbert AJ, Swanson B, Kuan L, Page DT, Overly CC, Lein ES, Hawrylyca MJ, Hof PR, Hyde TM, Kleinman JE, Jones AR (2012) Large-scale cellular-resolution gene profiling in human neocortex reveals species-specific molecular signatures. Cell 149:483–496